PB-215 475

THE EFFECT OF SEWAGE AND WASTE CHARACTERISTICS ON OXYGEN TRANSFER COEFFICIENTS

W. W. Eckenfelder, Jr., et al

Manhattan College
Bronx, New York

October 1972

DISTRIBUTED BY:

NTIS

National Technical Information Service
U. S. DEPARTMENT OF COMMERCE
5285 Port Royal Road, Springfield Va. 22151

RG4694

PB 215 475

U.S. PUBLIC HEALTH SERVICE

PROJECT NO. RG4694

THE EFFECT OF SEWAGE AND WASTE CHARACTERISTICS ON OXYGEN TRANSFER COEFFICIENTS

Reproduced by
NATIONAL TECHNICAL
INFORMATION SERVICE
U S Department of Commerce
Springfield VA 22151

FINAL REPORT

by

W. Wesley Eckenfelder Jr.

and

Edwin L. Barnhart

CIVIL ENGINEERING DEPARTMENT
MANHATTAN COLLEGE
NEW YORK

THE EFFECT OF SEWAGE AND WASTE CHARACTERISTICS ON OXYGEN TRANSFER COEFFICIENTS

FINAL REPORT

Prepared by

W. W. Eckenfelder, Jr., Project Director
E. L. Barnhart, Research Assistant

Public Health Project No. RG 4694

Sponsored by

U.S. PUBLIC HEALTH SERVICE
Division of Research Grants & Fellowships
Federal Security Agency
Bethesda, Maryland

Conducted by
Civil Engineering Department
MANHATTAN COLLEGE
New York, N. Y.

October, 1962

TABLE OF CONTENTS

Abstract

Acknowledgement

List of Figures

Introduction

Nature of Aeration and Oxygen Transfer

Experimental Apparatus and Procedures

Experimental Procedure for the Determination of $K_L a$ in the Bubble Column

Sample Data Calculation

Presentation and Discussion of Results

Conclusions

Nomenclature

Bibliography

Appendix 1 - Analytical Methods

Appendix 2 - Summary of Experimental Data

ABSTRACT

This report describes a series of experiments on the measurement of the overall oxygen transfer coefficient and the liquid film coefficient in solutions of surface active materials. Methods for measuring dissolved oxygen under test conditions and the procedures determining the liquid film coefficient, K_L, are described. A study of the effect of temperature on the overall oxygen transfer coefficient and the liquid film coefficient is presented. The effect of this temperature in various concentrations of an organic acid was also evaluated.

The overall oxygen transfer coefficient is influenced both by the liquid film coefficient and the interfacial area-volume ratio, A/V. Changes in solution, surface tension, viscosity and density still affect both of these factors resulting in an increase of degrees in the overall coefficient. At low concentrations of surface active agent the coefficient is reduced from that of the value of water, while at high concentrations the coefficient may increase to a value greater than that of water. The data obtained in this project indicate that the magnitude of the increase or decrease depends in part on the aerating device. The addition of defoaming agents may either increase or decrease the overall coefficient depending on the chemical nature of the defoamer.

The overall coefficient, K_La, was observed to increase 2% per degree and the liquid film coefficient, 2.8% per degree centigrade temperature rise over a temperature range of 10^o to 40^oC.

ACKNOWLEDGEMENT

This investigation was supported by a Research Grant from the Division of Research Grants and Fellowships of the National Institute of Health, United States Public Health Service, under Contract No. RG-4694. Experimental work was conducted at the Sanitary Engineering Laboratory at Manhattan College under the direction of W. Wesley Eckenfelder, Jr., Associate Professor of Civil Engineering.

The experimental work summarized in this report is the result of four years of a research program entitled "The Effect of Sewage and Waste Characteristics on the Oxygen Transfer Coefficient in Biological Oxidation Processes". The initial phases of the work were concerned with the development of satisfactory methods of oxygen measurement under the proposed test conditions and the construction of a suitable aeration unit. Early work studied the variation in oxygen transfer rate in solutions of peptone and sodium stearate using an aloxite diffusor stone. The last two years of the project utilized a standardized nylon spinnerette which yielded a more reproducible bubble pattern. During this phase of the project, the oxygen transfer characteristics were measured in dilute solutions of peptone, sodium lauryl sulfate, caproic, heptanoic and octanoic acids. A detailed study of the effect of temperature on the oxygen transfer coefficient was also conducted using the nylon spinnerettes.

As a result of this project, four papers were presented and published summarizing the various phases of the research.

1. Eckenfelder, W. W., Jr. and Burris, C. T., "Polarographic Measurement of Dissolved Oxygen", Special Technical Publication No. 219, American Society for Testing Materials, 1957.
2. Eckenfelder, W.W., Jr.. "A Correlation of Variables Affecting the Absorption of Oxygen from Gas Bubbles in Water" presented 48th Annual Meeting, American Institute of Chemical Engineers, Salt Lake City, Utah, Sept. 1958.

3. Eckenfelder, W. W., Jr. "Factors Affecting the Aeration Efficiency of Sewage and Industrial Wastes", Proc. 13th Industrial Waste Conference, Purdue University, May 1958.

4. Eckenfelder, W.W., Jr. and Barnhart, E.L., "The Effect of Organic Substances on the Transfer of Oxygen from Air Bubbles in Water" presented at the Forty-Second National Meeting, American Institute of Chemical Engineers, Atlanta, Georgia, February 1960.

The investigators wish to express their appreciation to the many under-graduate Sanitary Engineering students who worked on this project over the past four years.

LIST OF FIGURES

1. Relation Between Liquid Film Coefficient and Bubble Diameter.
2. Correlation of Bubble Aeration Data.
3. Experimental Apparatus.
4. Comparison of Surface Tension Methods.
5. Relation Between $K_L a$ and Air Flow for Solutions of Various Concentrations of Peptone - Aloxite Stone Diffusor.
6. Variation of Bubble Diameter with Peptone Concentration - Aloxite Stone Diffusor.
7. Variation of the Transfer Ratio, Alpha with Concentration of Peptone - Aloxite Stone Diffusor.
8. Oxygen Transfer in Solutions of Various Concentrations of Peptone - Nylon Spinnerette.
9. Relation Between $K_L a$ and Air Flow for Solutions of Various Concentrations of Sodium Stearate.
10. Variation of the Transfer Ratio, Alpha, with Concentration of Sodium Stearate - Aloxite Stone Diffusor.
11. Relationship Between $K_L a$ and d_B and Air Flow for the 0.035 mm Spinnerette.
12. Relationship Between G_S and d_B for the Nylon Spinnerettes.
13. Relationship Between the Overall Transfer Coefficient, $K_L a$, and Gas Flow for the Nylon Spinnerettes.
14. A Typical Relationship for the Effect of Temperature on Oxygen Transfer.
15. Relationship Between the Overall Transfer Coefficient, $K_L a$, and Temperature.
16. Relationship Between Liquid Film Coefficient, K_L and Temperature.
17. Correlation to Develop End Effects for the Aeration Column.
18. End Effects from the Data of Other Investigators.
19. Oxygen Transfer Characteristics in Dilute Solutions of Sodium Lauryl Sulfate.
20. Oxygen Transfer Characteristics in Dilute Solutions of Heptanoic Acid.
21. Oxygen Transfer Characteristics in Dilute Solutions of Various Organic Acids.

Introduction

The increasing use of aerobic biological processes for sewage and industrial waste treatment have stimulated investigations of the mechanism governing oxygen transfer in these systems. Oxygen transfer is primarily accomplished by the use of diffused bubble aeration or by mechanical aeration. While it has been known for a long time that the nature of a sewage or a waste markedly influenced the rate of oxygen transfer, very little quantitative information is available on the factors governing these influences. The oxygen transfer rate is also influenced by variations in waste temperature, by the use of defoaming agents and by variation in solids levels in the aeration tank. It is the purpose of this research project to study the variables affecting changes in oxygen transfer characteristics in sewage and industrial wastes.

THE NATURE OF AERATION AND OXYGEN TRANSFER

Aeration is a process involving mass transfer between a gas (air) and a liquid (water) when a driving force is created by a departure from equilibrium. In the diffusion process it is assumed that a dynamic equilibrium will exist at the interface itself. Since no concentration buildup can occur at the interface in steady state transfer, the diffusional resistances on the gas side and the liquid side can be considered in series and the controlling rate will be that which offers the greatest resistance to diffusion. It can be shown (1) that in the case of slightly soluble gases such as oxygen the controlling resistance occurs in the liquid film. In commercial aeration systems the fluid is in a turbulent state beyond the laminar film. Since the eddy diffusivity is many times the molecular diffusivity, the concentration may usually be considered uniform in the bulk of the liquid.

The transfer relationships can be developed from Ficks Law:

$$N_a = \frac{Dg}{z_g} (pg - pai) = \frac{D_L}{z_L} (Cai - Cs) \qquad (1)$$

When the liquid film offers the controlling resistance, and the interfacial concentration, C_{ai}, is assumed as saturation C_s, Equation (1) can be expressed:

$$N_A = D_L / z (C_s - C_L) = K_L (C_s - C_L) \qquad (2)$$

Equation (2) can be re-expressed in concentration units:

$$N_A = \frac{dw}{Adt} \text{ and}$$

$$\frac{1}{V}\frac{dw}{Adt} = \frac{1}{V}\frac{D_L}{z}(C_s - C_L) = \frac{dc}{dt} = K_L a (C_s - C_L) \qquad (3)$$

where

$$K_L a = K_L . A/V$$

Since it is usually difficult to measure interfacial areas in bubble aeration, $K_L a$ is frequently employed as the overall transfer coefficient to define the aeration process.

It is apparent from the foregoing that changes in the oxygen transfer rate will be reflected by changes in the mass transfer coefficient $K_L a$. In order to interpret the specific nature of changes in transfer rate it is necessary to differentiate between changes in the liquid film coefficient K_L and the interfacial area - volume relationship A/V.

The Liquid Film Coefficient K_L

Whitman and Lewis (2) developed a two-film theory which assumes, that at the interface, thin films of gas and liquid exist through which the oxygen must pass by molecular diffusion.

According to the two-film theory K_L can be defined as D_L/z. It can be further postulated that the thickness of the laminar layer, z, will decrease with increasing fluid turbulence, thus increasing KL. Indirect calculations of z have shown a variation of 0.2 cm in still water to .001 cm under turbulent conditions of bubble aeration (3).

Higbie (4) and later Dankwertz (5) related the liquid film coefficient to the square root of the product of the diffusivity and the time of surface renewal. This time is related to the velocity of the air bubble relative to the water. Dankwertz (5) determines an average rate of surface renewal and Higbie (4) evaluates the rate at any instant and then averages this rate over a selected time interval.

Higbie (4) defined K_L

$$K_L = \sqrt{\frac{4D_L}{\pi t'}} \qquad (4)$$

and Dankwertz (5) as

$$K_L = \sqrt{D_L/t'} \qquad (5)$$

The time, t', in Equations (4) and (5) is related to the rate at which layers of water molecules adjacent to the air bubbles are replaced by layers from the body of fluid. Pasveer (6) defined K_L as shown in Equation (4) from an integrated form of Stefans' equation.

For the transfer of oxygen from air bubbles in a column of water, the interfacial area - volume ratio will depend on the total area of the bubbles passing through the water and on the exposed surface at the top of the column. The overall transfer coefficient K_La will be the product of this ratio and the liquid film coefficient as previously defined.

Bubble Aeration

In diffused aeration, air bubbles are formed at an orifice from which they break off and rise through the liquid, finally bursting at the liquid surface. Oxygen transfer occurs during each phase of the bubble's life. As the bubble emerges from the orifice the absorption rate is very high. The air-water interface is continuously replenished during bubble formation resulting in a high surface renewal rate. When the bubble reaches its terminal velocity the transfer rate is constant as it rises through the liquid. The effective film thickness and the rate of surface renewal will vary with the bubble velocity and hence the mass transfer will be related to the velocity of the bubble, v_B. relative to the liquid. In aeration tanks where the liquid is in motion, the transfer process is complicated by eddy currents which result in irregular bubble movement.

The water surface will be continually renewed by the air bubbles bursting as they rise to the surface and shed an oxygen saturated film into the surface layers. Velocity gradients will also be induced

at the surface through fluid turbulence generated by the rising bubbles resulting in additional surface reaeration. To account for the three transfer phases Equation (2) can be modified:

$$N=k_{L(f)}A_f(C_{sb}-C_b) + k_{L(b)}A_b(C_{sM}-C_M) + k_{L(s)}A_S(C^*-C_n) = K_LA(C_s - C_L)$$

The liquid film coefficient during bubble formation and release is higher than that created by the rising bubbles. It may therefore be expected that the overall liquid film coefficient, K_L, will vary inversely with liquid depth.

Various attempts have been made to independently evaluate $k_{L(f)}$, $k_{L(b)}$, and $k_{L(s)}$. The coefficient for rising bubbles varies over the surface of the bubble. Adeney and Becker (7) showed that air bubbles rising at a velocity of 9 cm/sec exhibited a liquid film coefficient of 32 cm/hr at the side surface and 230 cm/hr at the tip where higher surface renewal rates were caused by the surface drag. An average coefficient for rising oxygen bubbles 0.03 cm diameter of 45 cm/hr was determined by Pattle (8). Indirect calculations of the data of Pasveer (9) showed values for $k_{L(b)}$ to range from 25-115 cm/hr for a range in air bubble diameter of 0.076 - 0.118 cm.

Streeter et al (10) expressed the surface film coefficient, $k_{L(s)}$ as an exponential function of the liquid velocity at the surface. Values of $k_{L(s)}$ as high as 250 cm/hr have been reported for a highly turbulent aeration tank surface (11). While very little data is available on the film coefficient during bubble formation, Kountz (12) has indicated that as much as 30% of the total transfer occurs during bubble formation.

Extrapolation of data reported by Lamb[39] on oxygen transfer from fine bubble diffusors in an aeration tank showed that 25% of the total transfer occurred during bubble formation in a tank depth of 12 ft. This percentage varied with the air rate. For large bubble nozzles considerably less transfer occurred during bubble formation. A part of this investigation has been devoted to a study of end effects and the results are reported in the body of this report.

Bubble Velocity

The velocity and shape characteristics of air bubbles in water can be related to a modified Reynolds Number (13). At Re less than approximately 300, the bubbles are spherical and act as rigid spheres. The bubble rise is rectilinear or helical. Over a Re range of 300 - 4000 the bubbles assume an ellipsoidal shape and rise with a rectilinear, rocking motion. The bubbles form spherical caps at Re greater than 4000.

The rising velocity of the bubbles is increased at high air flows due to the proximity of other bubbles and resulting disturbances of the bubble wakes.

Bubble Size

The size of air bubbles released by diffused aeration devices is

related to both the orifice diameter and the air rate. At low air rates the bubble volume is directly proportional to the orifice diameter and the surface tension and inversely proportional to the liquid density. The bubble size produced will result from a balance of the buoyant force separating the bubble from the orifice and the shearing force necessary to break the surface tension across the orifice (14). McKeown [40] has shown that at low air rates the bubble diameter is constant with increasing air flow and the frequency of bubble formation is proportional to air flow. At intermediate air rates both the frequency of formation and the bubble diameter vary with air flow. Over the range of air rates normally encountered in aeration practice the mean diameter of bubble produced is an exponential function of the gas rate and the frequency of bubble formation remains constant.

$$d_B \sim G_s^{\,n} \qquad (7)$$

Data from four diffusers employed by Pasveer (9) showed the exponent n to vary from 0.10 to 0.44. Typical data is shown in Figure 1.

The liquid film coefficient will increase with increasing bubble size up to a bubble diameter of approximately 0.2 cm. This increase will approximately parallel the variation in terminal bubble velocity with bubble size. Bubble diameters in excess of 0.2 cm yield a decreasing value of K_L. This relationship is shown in Figure 1.

From Equation (1) it is seen that the rate of oxygen transfer is proportional to the oxygen saturation deficit ($C_{ai} - C_L$). If the dissolved oxygen content C_L is maintained constant then the transfer will be directly related to the concentration at the interface C_{ai}. Since the interfacial concentration cannot be measured it is assumed that the interface will correspond to saturation and that $C_{ai} = C_s$. Direct solution of Equation (1) considers C_{ai} and A constant over the operating conditions under consideration. Actually both C_{ai} and A will vary as the bubble rises through the tank liquid due to a change in hydro static pressure on the air bubble and due to absorption of oxygen from the bubble. These two factors tend to produce a compensatory effect and for most conditions average values of C_{ai} and A are employed, corresponding to conditions at the midpoint of the tank depth.

Ippen and Carver (14) computed the interfacial equilibrium concentration at the diffuser outlet and the surface respectively as:

$$C_{ai\ (bottom)} = C^* \left[\frac{P_B + P_H + P_\sigma - p_v}{760 - p_v} \right] \qquad (8)$$

and

$$C_{ai\ (surface)} = C^* \left[1 - O_2 \text{ absorbed } \frac{P_B - p_v}{760 - p_v} \right] \qquad (9)$$

It can be shown that for bubbles one mm or larger the surface tension pressure P_σ can be neglected.

If the barometric pressure and water vapor corrections are neglected, Oldshoe (15) showed that C_s (average) is:

$$C_s = C^* \left[\frac{P_H}{29.4} + \frac{O_t}{42} \right] \qquad (10)$$

At 20°C in a tank of 12 ft. depth and bubble diameters of 3.0 mm and 0.2 mm the mean saturation value of oxygen, C_s, computed by Equations (8) and (9) and Equation (10) is 10.29 and 10.40 respectively. For most purposes the use of Equation (10) is justified.

Correlations of Mass Transfer Data

Several efforts have been made to correlate mass transfer data from bubble aeration systems. Hammerton and Gamer (16) showed that the Frossling Equation could be employed to correlate oxygen transfer data when the bubbles acted as rigid spheres and before bubble circulation started (0.02 cm diameter)*. This correlation was also applied to those cases where the presence of contaminants prevented bubble circulation. Over a bubble diameter range of 0.3 - 0.8 cm, Higbie's formula was found to give a reasonable correlation. The time of surface renewal was estimated to be that required for the bubble to rise one diameter. Camp (17) developed a similar relationship from the data of Ippen and Carver (14) which employed a modification of the Dankwertz equation:

$$K_L = m\sqrt{D_L \, {}^{V_B}/_{d_B}} \qquad (11)$$

Effects due to variations in submergence depths were not considered in the above correlations.

Quigley, Johnson and Harris (18) developed a relationship for large bubbles discharged from submerged orifices on perforated gas absorption plates at low submergence depths:

$$K_L = C \, {}^{V}/_{d_B} \cdot 1/S_c^{\,2/3} \qquad (12)$$

The liquid film coefficient for oxygen transfer from a moving surface under turbulent conditions has been shown by O'Connor (19) to be:

$$K_L = \sqrt{\frac{D_L V_L}{h}} \qquad (13)$$

None of the aforementioned equations have correlated oxygen transfer data over a wide range of submergence depths and bubble characteristics. It has been previously shown that the liquid film coefficient, K_L, increases with decreasing depth due to the three phases of the transfer process. Transfer coefficients developed for various depths and bubble sizes have been correlated to the Sherwood Number and the Reynolds Number (4) as shown in Figure 2. The relationship developed in Figure 2 correlates well for liquid submergence depths in excess of 3 ft.

*$N = 4 \; D_L \frac{MP}{RT} r_B \; 1 + 0.276 \, S_c^{\,0.33} \, R_e^{\,0.50}$ ...

The general relationship obtained for these data is:

$$\frac{K_L d_B}{D_L} \cdot h^{1/3} = C\,(Re)\,(Sc)^{1/2} \qquad (14)$$

Rearranging Equation (14) shows the overall liquid film coefficient for air bubbles rising through a column of water to be:

$$K_L = \frac{C\,v_B}{h^{1/3}} \cdot \frac{1}{Sc^{1/2}} \qquad (15)$$

Considered in light of the relationships developed by Higbie and Dankwertz the rate of surface renewal will be directly proportional to the square of the velocity and inversely proportional to the liquid viscosity.

Equation (14) was developed over a range of Reynolds Number of 50 to 500 and a range of depth of 0.6 ft - 12 ft. For Reynolds Numbers in excess of 5000 Quigley, Johnson and Harris (18) showed the surface renewal rate to be inversely proportional to the bubble diameter and the fluid viscosity.

Overall Mass Transfer Coefficients

When considering the performance of commercial aeration equipment it is convenient to consider the aeration process in terms of overall mass transfer coefficients. The mass transfer is described by the equation:

$$N/V = K_L \frac{A}{V} (C_s - C_L) = K_L a\,(C_s - C_L)$$

In bubble aeration processes A/V is equal to:

$$\frac{6\,G_s h}{d_B v_B V} + C\left(\frac{1}{h}\right) \qquad (16)$$

The first term expresses the air-volume relationship for the bubble surface and the second for the tank surface.

For the deep depths normally employed in aeration practice (10 - 15 ft.) the term 1/h becomes small with respect to the bubble surface and can usually be neglected. For example, in an aeration tank of 15 ft. depth with an air flow of 20 scfm/1000 cu ft. and a bubble diameter of 0.1 inches, A/V for the bubbles will be 1.8 and for the surface 0.067. (1/h) would represent a smooth surface while actually the interfacial area will be considerably greater, due to the high degree of surface turbulence. To compensate for this, a constant C is included in Equation (16). C is greater than 1.0. Equations (15) and (16) can be combined to define the overall coefficient $K_L a$ where the surface effect on the A/V ratio is neglected:

$$K_L a = \frac{C' h^{2/3} G_s}{V d_B^{1/2} S_C} \qquad (17)$$

Combining Equation (8) with Equation (17) where the exponent n relates to both the variation in bubble size with air rate and turbulence as influenced by tank geometry gives:

$$K_L a \cdot V = C'' G_s^{(1-n)} \quad 2/3 \qquad (18)$$

Equation (18) may be employed to characterize the performance of aeration devices in water.

Effect of Gas Rate on Oxygen Absorption

The volume of bubbles produced from small orifice diffusion units is related to the orifice size. For Carborundum plates (20) the diameter of air bubbles has been found to vary from 0.2 cm - 0.43 cm over a permeability range of 40 - 120[1].

The mean diameter of bubbles produced at high air rates is an exponential function of air rate as shown by Equation (8). In evaluating aeration equipment it is more convenient to consider the exponent (1-N) as related to the overall coefficient $K_L a$ (Equation 18). The exponent will also reflect the effect of tank turbulence and geometry.

For small orifice diffusion units (carborundum plates and tubes, seran tubes, etc.) the exponent is less than 1.0 indicating an increasing bubble size over a range of air flow of 1 scfm to 4 scfm for Carborundum plates. Over a wide range of bubble fineness and dispersion Gaden and Hixon (21) showed the exponent (1-n) to vary from 0.33 - 0.82. For these devices, when (1-n) is less than 1.0, the absorption efficiency decreases with increasing air rate.

In the case of the sparjer and discfuser units with increasing air rates, tank turbulence tends to redivide larger bubbles into smaller bubbles increasing both the surface renewal rate and the A/V ratio. When this occurs, the gas rate exponent (1-n), may be greater than 1.0 resulting in an increasing transfer efficiency with increasing gas rate. This phenomenon, however, is related to the tank geometry and the location of the diffuser unit.

Effect of Submergence Depth

The exponent of 2/3 on the submergence depth as determined from the aeration of water in tall columns has been found to vary from this value in commercial aeration tanks depending on the geometry of the tank and location of the air diffuser in the tank. Over the range of depths employed the overall coefficient $K_L a$ in industrial systems can be related to an exponential function of depth. The exponent on depth, m, has been experimentally determined for several diffused aeration systems and is summarized below. There is some experimental evidence that the exponent (1 - m) for turbine aeration approaches 1.0, indicating no change in absorption with tank depth. This is not unreasonable when one considers that the fluid regime of a turbine aeration system approaches a homogeneous condition at all depths.

[1]Permeability is defined as a cfm of air per sq. ft. of diffuser surface at 70°F, 25% relative humidity and a pressure loss of 2 inches of water.

Effect of Depth on the Oxygen Transfer Rate Coefficient

System	Exponent (1 - m)
Diffusors in still water column	0.67
Plate diffusors[1]	0.71 - 0.77
Diffusair Sparjers	0.78
Aloxite Tubes[2]	0.45
Impingement (2)	0.65

---

[1] date of King(20)
[2] date of Dreier(22)

Tank Circulating Velocities

The rate of interfacial renewal in an aeration tank is proportional to the velocity of the bubble relative to the tank liquid. High circulating velocities will produce large values of the liquid film coefficient, K_L. In addition, interfacial renewal rates at the tank surface will be related to velocity gradients at the surface.

The surface velocity measured by King (20) in a 34 ft. wide aeration tank was found to vary from 4.3 ft/sec. above the diffusor plates to 2.1 ft/sec. near the side wall opposite the plates. For all of the aeration devices included in these studies the liquid velocities near the surface ranged from 2.0 to 4.0 ft/sec. and from 0.5 to 2.0 ft/sec. at greater depths.

A traverse made of dissolved oxygen values at various points in the aeration tank described above showed the dissolved oxygen to be substantially constant throughout the tank. It is therefore reasonable to expect that at the turbulence levels encountered in commercial aeration practice, no concentration gradient will exist in the aeration tank itself.

Effect of Temperature

The overall transfer coefficient K_La will be affected by changes in operating temperature. Temperature influences the diffusivity of oxygen in water as well as other physical variables in the aeration process. Temperature coefficients have been derived by investigators for various types of transfer processes. Differences have been observed in the coefficients for surface and diffused aeration. Since both surface tension and viscosity of water are temperature functions the surface area and time of contact of bubbles in water are probably influenced by temperature.

Downing and Truesdale (23) found an average temperature coefficient of 2 percent per ^{o}C with a range of 1.9-3.7 percent per ^{o}C for water stirred under various conditions. In a later study (24) these investigators found an average coefficient of 1.5 percent per ^{o}C for water flowing in an open channel. By comparison, Streeter et al (10) reported a coefficient ranging from 4.1 - 4.7 percent per ^{o}C. A range in coefficient for diffused aeration of 1.6 - 3.5 percent per ^{o}C has been reported by Philpott (25).

Energies of activation have ranged from 1.2 - 3.3 Kcal/g. mole. Carpani and Roxburgh (26) reported an activation energy of 1.2 Kcal/g. mole for stirred aeration of water. Bartholomew et al (27) reported an activation energy of 4.2 kcal/g mole. O'Connor (19) has employed a modification of the Stokes - Einstein equation to define the effect of temperature on $K_L a$. From data on wetted wall columns Haslam et al (29) derived the relationship: $K_L(t) = K_L(20^{o}C) \cdot (T/293)^{4}$. Pasveer (6) showed K_L at any temperature to be related to the square root of the ratio of K_L at $10^{o}C$ and the operating temperature. King (20) employed the relationship $K = K_L \cdot 1.024^{T}$. Several of the formulations proposed are summarized below:

Relative Effects of Temperature
on the Oxygen Transfer Coefficient

Temp. ^{o}C	0	10	20	30	40	E	% K
Stokes-Einstein	0.724	0.867	1.00	1.135	-	1080	1.37
Haslam	0.758	0.867	1.00	1.132	1.310	1080	1.38
Pasveer	0.690	0.832	1.00	1.215	1.454	1253	1.91
Streeter	--	0.85	1.00	1.17	--	1000	1.60
King	0.650	0.790	1.00	1.265	1.580	1520	2.32
Barth - olomew	0.572	0.765	1.00	1.245	1.540	4200	2.42
Carpani-Roxburgh						1200	

Note: % K is the percent increase of the oxygen transfer coefficient per degree Centergrade.

Effect of Waste Constituents

Various investigators have found that the oxygen transfer rate is altered from that in pure water in the presence of surface active agents or other contaminants. It has been further found that the magnitude of the change depends on the concentration of the contaminant and to a large extent on the nature of aeration and the characteristics of the aeration surface. This effect is primarily due to an interfacial adsorbed film which depends upon the type of surface active agent, the number of carbon atoms, and the molecular configuration and the time necessary to reach adsorption equilibrium. Those surface active agents which quickly reach equilibrium will have a much more profound effect on oxygen transfer than those which slowly reach equilibrium. In like manner a continuously renewed surface will exhibit less effect than will a long exposure as occurs as a bubble rises through a deep tank.

For example Downing and Truesdale (23) showed that the addition of 1 ppm of alkylbenzene sulfonate to sea water reduced K_L from 10.25 to 5.1 cm/hr through a surface ruffled by air jets while the same concentration in tap water agitated by waves 8 cm high only caused a reduction of 24.5% in K_L (21.6 - 16.3 cm/hr). Holroyd (11) has shown that in the presence of surface active agents the most significant reduction in K_L occurs at the bubble surface. A less severe depression of K_L occurs at the bubble surface. A less severe depression of K_L was observed at the stagnant film surface and the least depression at the heaving water surface. The reduction in K_L is attributed to an adsorbed layer of the surface active agent at the air liquid interface. At the heaving water surface the short life of any interface restricts the formation of an adsorbed film. A diffusion barrier at the interface was also defined by Bartholomew et al (27). Ippen and Carver (14) showed that a reduced shear at the bubble boundary and a slower rate of bubble rise due to a smaller bubble size in the presence of a surface active agent reduced the rate of surface renewal. McKeown and Okun [40] have postulated that the maximum resistance to gas transfer due to surface active agent adsorption occurs at the critical micelle concentration. This is defined as the concentration at which the solution forms colloidal aggregates by the association of molecules or ions. The critical micelle concentration is characterized by an abrupt change in slope of the surface tension-concentration curve.

The interfacial area for transfer (A/V) will also be influenced by surface active agents in bubble aeration. Gaden (21) showed that it is possible for very small quantities of surface active agents to alter the foaming properties of the liquid sufficiently to change the effective bubble size as much as 100 times. It was shown (14) that bubble size varied inversely with detergent concentration.

Experimental Apparatus and Procedure

An aeration column 5 cm. in diameter with a total liquid depth of 110 cm. was employed in these investigations. The column was jacketed by a second column 9 cm. in diameter to provide a circulating water bath for temperature control. Air was diffused through a nylon spinnerette 3/4" in diameter with 20 holes each 35 in diameter distributed over the surface. This device produced bubbles ranging from 0.12 to 0.16 cm. in diameter in pure water. The air flow was metered through a rotometer. Samples for dissolved oxygen measurement were withdrawn from a tap located 80 cm. from the base of the column. The experimental appartus is shown in Figure 3 . A series of oxygen transfer studies were also conducted employing an aloxite diffusor stone. The bubbles generated from this diffusor ranged in size from 0.03 to 0.06 cm. in diameter.

Dissolved oxygen was measured with a manual polarograph with a dropping mercury electrode. The operating voltage for each substance studied was determined from a current-voltage curve. In each case the first oxygen plateau was used. Potassium chloride was added to each sample as a supporting electrolyte. For each series of test runs the polarograph was calibrated against the Winkler dissolved oxygen.

In order to define the bubble characteristics glass ports were placed in the column at 15 and 95 cm. above the spinnerette. The velocity and diameter of the bubbles were measured by photographing with a 35-mm. Reflex camera. A speed of 1/500 sec. was used to determine bubble diameter. A speed of 1/50 sec. was used to obtain streaks from which the bubble velocity was determined. The photos were developed as strip film and mounted as slides, and the average bubble characteristics were measured by projection on a screen.

Surface tension for the various substances and concentrations was determined by two methods. The equilibrium surface tension was determined by the platinum ring method with a tensiometer. The dynamic surface tension was determined by the method of maximum bubble pressure ( ). Figure 4 shows a comparison of the results of the two methods for various concentrations of sodium lauryl sulfate.

EXPERIMENTAL PROCEDURE FOR DETERMINATION OF KL_a IN BUBBLE AERATION COLUMN

1. Calibrate Polarograph:
   Record instrument zero reading. Vigourously shake 1% KCl solution sample in stoppered bottle; take current reading and temperature. Three or four readings after successive shaking should be obtained so as to insure sample saturation. Sample should then be purged with nitrogen gas and current recorded. This is also repeated so as to obtain lowest possible reading. The calibration factor for the polarograph is calculated as shown on sample calculation sheet.

2. De-aerate sample in column by purging with nitrogen gas (5 - 10 minutes).

3. After the nitrogen purge withdraw sample in beaker and place in polarograph. Measure residual current and temperature.

4. Introduce air at specified rate through diffuser stone. Start a stop-watch simultaneously with the air flow.

5. At two-minute intervals withdraw samples in beaker and place in polarograph. Record current and temperature. When new sample is withdrawn, it should be replaced with previous sample.

6. The sampling is continued for 10 - 12 minutes.

7. Calculate saturation value of sample by shaking sample in stoppered bottle and recording current reading and temperature. This procedure should be repeated several times to insure saturation.

8. Calculate the dissolved oxygen, C_L, at the various time intervals by the procedure as shown in the sample calculations.

9. Calculate the saturation value C_s.

10. Plot log $(C_s - C_L)$ vs. time.

11. Compute K_La as the slope of the log plot.

12. Repeat procedure using 1% KCl.

13. Compute α $(=K_La \text{ sample}/K_La \text{ 1\% KCl})$.

SAMPLE CALCULATION

Applied Voltage - 0.6 Volts

Solution - 1% KCl Standard

Purge Current - 4.0 @ 27°C

Saturation Current - 48.4 @ 27°C

D.O. of 5000 ppm CL- @ 27 = 7.67 ppm

D_t (Diff. in Readings) = (D_{st}) - (D_{purge})

= 48.4 - 4.0)

D_t = 44.4

All data is corrected with respect to a temperature of 20°C. This correction is applied as follows:

$$D_{20} = D_t \; 1 + .014 \; (20 - t)$$

In this case D_{20} = 44.4 1 + .014 (20 - 27)
= 44.4 (.902)
= 40.1

$$f \text{ (polarograph factor)} = \frac{\text{D.O.Saturation}}{D_{20}} = \frac{7.67}{40.1} = 0.191$$

at a Temp = 26° f' = f x Temp Corr = 0.191 x .916 = 0.175

1% CL Sat @ 26° = 7.81 ppm

Time (min)	Current Reading-Purge D_t	D.O ppm	Deficit C_s-C_L
0	-	-	7.81
2	14.6	2.55	5.26
4	24.0	4.20	3.61
6	30.6	5.35	2.46
8	34.6	6.06	1.75
10	38.0	6.61	1.20
12	40.8	7.11	0.70

$D.O = D_t \times f^1$

= 14.6 x 0.175 = 2.55

Def = 7.81 - 2.55 = 5.26

PRESENTATION AND DISCUSSION OF RESULTS

The first phase of this project was devoted to an evaluation of methods for the measurement of dissolved oxygen by chemical and polarographic methods. These results are discussed in this report under "Analytical Methods".

A second phase of study considered the variations in the oxygen transfer rate coefficient in solutions of various concentrations of peptone and sodium stearate. Oxygen transfer was accomplished by aeration with an aloxide diffuser. A study was made to evaluate the effects of several commercial defoaming agents on the oxygen transfer rate coefficient.

The variation in oxygen transfer rate in solutions of various concentration of caproic, heptanoic and octanoic acid were investigated. In these studies a nylon spinnerette was used as an air diffuser. The spinnerette had uniformly drilled holes and yielded a more constant bubble size distribution. In order to determine the effects of salts on the oxygen transfer rate a series of investigations were conducted to determine the transfer rate in various concentrations of potassium chloride. The transfer rate in the presence of a common syndet, sodium lauryl sulfate was also investigated.

The effect of temperature over the range of 10°C to 40°C on both the liquid film coefficient K_L and the overall transfer coefficient K_La was evaluated using the spinnerettes.

Oxygen Transfer in Peptone Solutions

Peptone was selected as a test solution since its constituents are commonly found in sewage and many industrial wastes. Peptone is a high molecular weight organic and will lower the surface tension of water.

The oxygen transfer coefficient, K_La, was determined for concentrations of peptone from 5 ppm to 20,000 ppm. The air flow to the column was varied from 9 cc/min. to 50 cc/min. The temperature was maintained constant at 21 - 22°C.

The transfer coefficient, K_La, increased exponentially with increasing gas flow according to Equation (18). For any one series of runs the exponent, n, was a constant for both the 1% KCl and solutions of various concentrations of peptone. Over a period of one year, however, for individual test series, the exponent, n, was found to vary from 0.63 - 0.95. This may be attributed to variations in the characteristic of the diffusion device. A typical set of test results are shown in Figure 5 . The overall correlation of the data was made by comparing the value of K_La/G_s^n for the peptone solution to a corresponding value of K_La/G_s^n for the 1% KCl solution. These data are summarized in Table 6.

Average bubble diameters were determined for each of the peptone concentrations by methods previously described. Increasing the concentration of peptone resulted in a smaller bubble size. This relationship is shown in Figure 6 . It was observed that at low concentrations of peptone the transfer coefficient was reduced below that for a

solution of 1% KCl. At high concentrations, the transfer coefficient increased to a value greater than that in the 1% KCl solution. The minimum in transfer rate was found at a peptone concentration of 2500 ppm. This relationship is shown in Figure 7 .

Since the bubble diameter decreased with increasing concentration of peptone, the bubble velocity will also decrease. This will result in a decrease in the liquid film coefficient, K_L, at high peptone concentrations. The reduction in K_L is compensated by an increase in A/V in the overall transfer coefficient. Later studies on oxygen transfer in peptone solutions using the spinnerette did not show the high K_La values at high peptone concentrations. The difference in these results can only be attributed to a large increase in A/V in the case of the Aloxite stone as compared to the spinnerette. Figure 8.

Oxygen Transfer in Sodium Stearate Solution

Sodium stearate is a surfactant which will reduce the surface tension of water in small concentrations. The oxygen transfer rate was measured in solutions of sodium stearate in concentrations up to 500 ppm and compared to the value for a 1% KCl solution.

An initial series of experiments were conducted to establish that the transfer ratio, α , was independent of air flow. These results are shown in Figure 9 . Since air flow was not found to be a factor in the determination of α , all runs were made at a constant air flow of 25 cc/min.

The transfer ratio, α , decreased with increasing concentration of sodium stearate. The surface tension likewise decreased with increasing concentration. Difficulties with the photographic arrangement prevented the measurement of bubble sizes during this series of test runs. The relationship between the transfer coefficient ratio and concentration of sodium stearate is shown in Figure10 .

Effect of Defoaming Agents on the Oxygen Transfer Coefficient

The tendency of many organics and surfactants to foam when aerated necessitates the use of defoaming agents. A series of tests were conducted to evaluate the effect of five commercial defoaming agents on the oxygen transfer rate in 1% KCl solution and in a solution of 500 ppm of peptone. These data are summarized in Table I . Types A and E are silicone base and types B, C, and D, are oil base defoaming agents. The coefficient α was computed as the ratio of K_La in the test solution to K_La α was computed as the ratio of K_La in the test solution to K_La of 1% KCl solution at the same air flow. In all of these studies α was independent of air flow. α represents the change in transfer rate in a 500 ppm peptone solution following the addition of a defoamer.

Types A and B resulted in a decrease in transfer rate in water up to a concentration of 10 ppm. Types C and D resulted in an increase in transfer rate in water over the same concentration range. The silicone base defoamer, type A, similarly reduced the transfer rate in the 500 ppm peptone solution. Type D also reduced the transfer rate in the peptone solution.

These studies indicate that the chemical nature of the defoaming agent will markedly affect the oxygen transfer characteristics of the solution. A future phase of this project will consider relationships between the chemical nature of the defoamer and its effect on the oxygen transfer rate coefficient.

Oxygen Transfer Characteristics of the Nylon Spinnerettes

The relationship between the overall oxygen transfer coefficient $K_L a$ and gas flow for the 0.035 mm spinnerette is shown in Figure 11. The relationship between bubble diameter and gas flow for this spinnerette is also shown in this figure. The average data relating bubble diameter to gas flow obtained for both the 0.035 mm and the 0.05 mm spinnerettes are summarized in Figure 12. As can be seen from Figure 12, there is no clear-cut distinction between the bubbles produced by the 0.035 mm spinnerette and the 0.05 spinnerette. The relationship between $K_L a$ and gas flow for all the data obtained on the two spinnerettes is summarized in Figure 13. It is similarly true that there is no clear cut distinction between the transfer rate for the two spinnerettes.

Effect of Temperature on Oxygen Transfer

Oxygen transfer studies were conducted on both water and a 50 ppm solution of heptanoic acid at temperatures of 10, 20, 30 and 40°C. The temperature in the aeration column was maintained by a continuous circulating water jacket. A typical set of results are shown in Figure 14. The effective temperature was evaluated on both the overall transfer characteristic $K_L a$ and the liquid film coefficient K_L. The temperature effects on the bubble diameter were also estimated by the methods previously described. The effect of temperature on $K_L a$ and K_L during this investigation were analyzed by regression analysis to obtain the line of best fit for each diffuser. Figure 15 shows the results obtained for the overall transfer coefficient $K_L a$. These data may be expressed by the relationship:

$$K_L a_t / K_L a_{20} = 1.020^{t-20}$$

This figure also includes data obtained by other investigators and for other aeration units. As can be seen from the plot, the type of diffusion unit seems to have no influence on the temperature coefficient. Figure 16 presents the results with variation of K_L with temperature. From a statistical analysis of these data the following relationship was developed:

$$K_{Lt} / K_{L20} = 1.028^{t-20}$$

The variation between the temperature coefficient of $K_L a$ and K_L undoubtedly reflects the effect of temperature on the bubble characteristics. The calculated ratios from the regression analysis for water and heptanoic acid are summarized below. The water data represents the results of 40 test runs and the heptanoic acid the results of 33 runs.

	Water	Heptanoic Acid
Temp.	Kl_t/Kl_{20}	Kl_t/Kl_{20}
10	0.75	0.77
20	1.0	1.0
30	1.28	1.29
40	1.7	1.68

End Effects

As previously mentioned, oxygen transfer during formation and surface disturbance are included in K_La, the overall transfer coefficient. It is possible, however, by making certain assumptions, to define the magnitude of such effects and to calculate a value of K_L for the rising bubble which will be independent of these effects.

From Equation 6

$$N = K_L(f)\ A_f(Csb-Cb) + K_{L(b)} A_b(Csm-Cm) + K_{L(s)} (C^*-Cn) = K_La(Cs-Cl)$$

If for the given experiment we assume that saturation is not significantly effected by depth and that the concentration of oxygen within the chamber is uniform (assuming a completely mixed system) then Equation 6 may be written:

$$N = K_{L(f)} Af(Cs-Cl) + K_{L(b)} A_b(Cs-Cl) + K_{L(s)} As(Cs-Cl) = K_LA(Cs-Cl)$$

or $$K_La_t \cdot V_t = K_La_{(b)} \cdot V_{(b)} + K_La_{(s)} \cdot Vt + K_La_{(f)} \cdot V_{(f)}$$

For a column of fixed surface area and reasonable depth, it is assumed that the total oxygen transferred during bubble formation and through surface aeration is constant for a given air flow and diffuser.

$$K_La_t \cdot V_t = K_La_{(b)} \cdot V_{(b)} + C_1$$

$$K_La = K_L\frac{A}{V}$$

$$K_La_t \cdot Vt = K_L\frac{A}{V_b} \cdot V_b + C_1$$

$$K_La_t \cdot V_t = K_LA + C_1$$

Where $A = \frac{6GsH}{d_BV_B}$

or $K_La \cdot V = K_L \frac{6GsH}{d_BV_b} + C_1$

K_L may therefore be calculated from the slope of the plot $K_La \cdot V$ vs $\frac{6GsH}{d_BV_v}$.

The intercept will reflect the quantity of oxygen transferred through end effects. The agreement of experimental data with this formulation is shown in Figure 17 . Figure 17 presents the data from the present study while Figure 18 shows the data of Ippen and Carver for a given air flow (88 cc/min).

From such plots the liquid film coefficient K_L during bubble rise may be calculated and the magnitude of the end effect of any system defined.

Oxygen Transfer Characteristics in Solutions of Various Surface Active Materials.

The effect of various concentrations of the organic acids caproic, heptanoic, and octanoic were determined using the nylon spinnerettes. These data are summarized in the Appendix B.

The variation in K_La, K_L and d_B with concentration of sodium lauryl sulfate is shown in Figure 19. The liquid film coefficient, K_L decreases rapidly at low concentrations of sodium lauryl sulfate. Above a concentration of 15 ppm K_L remains substantially constant up to a concentration of 50 ppm. The bubble diameter decreases with increasing concentrations of sodium lauryl sulfate. This contributes to an increase in the overall transfer coefficient K_La at high concentrations of the surface active agent.

A similar series of runs were made on N. heptanoic acid. The liquid film coefficient, K_L, initially decreased followed by a slight increase at high concentrations. The bubble diameter also decreased with increasing concentration which contributed to an increase in K_La at the higher concentrations of heptanoic acid. The average data for heptanoic acid is shown in Figure 20.

The effect of varying concentration of three organic acids on the liquid film coefficient, K_L is shown in Figure 21. It was not possible from these data to relate the oxygen transfer characteristics to the molecular weight of the acid.

CONCLUSIONS

From the results of this project, it may be concluded that:

1. The polarographic method for the measurement of dissolved oxygen may be employed for organic solutions in cases where the Winkler method is not applicable providing the proper operating voltage is selected. In some cases a supporting electrolyte is necessary.

2. The liquid film coefficient for the transfer of oxygen from air bubbles in water is directly proportional to the velocity of the bubble in the water and inversely proportional to the viscosity.

3. The overall transfer coefficient for air bubbles in water will vary 2% per degree centigrade change and the liquid film coefficient 2.8% per degree centigrade change over a temperature range of 10° to 40° C.

4. The overall transfer coefficient and the liquid film coefficient will decrease in the presence of dilute concentrations of surface active materials. Depending on the type of diffusor employed, the overall transfer coefficient may increase at high concentrations of surface active agent. This contributed to an increase in the inter-facial area-volume ratio, A/V.

5. Commercial defoaming agents may increase or decrease the oxygen transfer rate relative to that in water depending on the chemical nature of the defoaming agent and oxygen transfer characteristics in the presence of various surface active materials.

NOMENCLATURE

A - interfacial area for transfer

a - ratio of interfacial area to liquid volume

C, C', C'' ... constants

C_{ai} - oxygen concentration at the gas-liquid interface

C^* - oxygen saturation in water at atmospheric pressure

C_L - dissolved oxygen concentration in the liquid

C_s - saturation of oxygen in water or waste at the mean depth and average oxygen concentration in the gas phase

c, c', c'' ... exponents

D_L - coefficient of diffusivity of oxygen in water

d_B - mean diameter of air bubble

G_s - air flow, scfm

h - tank liquid depth

$k_{L(f)}$ $k_{L(b)}$ $k_{L(s)}$ - liquid film coefficient during bubble formation, bubble rise, and surface aeration respectively.

K_L - overall liquid film coefficient, cm/hr.

K_La - overall oxygen transfer coefficient, 1/hr.

m - depth exponent

N - rate of mass transfer per unit time

n - gas rate exponent

O_t - percent oxygen in air leaving the aeration tank

p - partial pressure

P_{ai} - partial pressure of oxygen at the gas liquid interface

P_g - partial pressure of oxygen in the gas phase

P_H - head of water over air diffusion device, psi

R_e - Reynolds Number $\frac{V_B d_B}{\quad}$

S_c - Schmidt Number - $\frac{\quad}{D_L}$

t - time

t' - time for interfacial renewal

NOMENCLATURE

V - volume of liquid under aeration

v_B - velocity of air bubble relative to tank liquid

z - thickness of interfacial gas or liquid film

BIBLIOGRAPHY

1. Treybal, R. E. "Mass Transfer Operations", McGraw Hill Book Co., New York, N. Y. (1955)

2. Lewis, W. K. and Whitman, W. C., Ind. Eng. Chem., 16, 1215, 1924

3. Haney, P. D., Jour. Amer. Water Works Assoc., 46, 353, 1954

4. Higbie, J., Trans. Am. Inst. Chem. Engrs., 31, 365, 1935

5. Dankwertz, P. V., Ind. Eng. Chem., 43, 1460, 1951

6. Pasveer, I., Sewage ind. Wastes., 26, 28, 1954

7. Adeney, W. E. and Becker, H. G., Phil. Mag., 38, 317, 1919 and 39, 385, 1920

8. Pattle, R. E., Trans. Inst. Chem. Engrs., 28, 27, 1950

9. Pasveer, A., Sew. and Ind. Wastes, 27, 10, 1130, (Oct. 1955)

10. Streeter, H. W., Wright, C. T. and Kehr, R. W., Sew. Wks. Jour., 8, 282, 1936

11. Holroyd, A., Water and San. Eng. (Br.) 3, 301, 1952

12. Kountz, R. R., Proc. 9th Ind. Waste Conf., Purdue Univ., 1954

13. Haberman, W. L. and Morton, R. K., Trans. Am. Soc. of Civil Engrs., 121, 227, 1956.

14. Ippen, A. T. and Carver, E., M. I. T., Hydrodynamics Lab. Tech. Rept. No. 7, May 1952; Tech. Rept., No. 14, 1955.

15. Oldshue, J. Y., Proc. 10th Ind. Waste Conf., Purdue Univ. p. 391, 1955

16. Hammerton, D. and Gamer, F. H., Trans. Inst. Chem. Engrs. (Br.) 32, 1954 Supplement

17. Camp. T. R., Proc. Amer. Soc. Civil Engrs., Jour. San. Eng. Div. 1227-9, April 1957

18. Quigley, C. J., Johnson, A. I. and Harris, B. L., Chem. Eng. Prog., Symposium Series, 51, 16, 1955

19. O'Connor, D. J. and Dobbins, W. E., Trans. A.S.C.E. 123, 641, 1958

20. King, H. R., Sewage Ind. Wastes, 27, 894, 1955, 27, 10, 1123, Oct. 1955

21. Gaden, E. L. Jr. and J. Hixon, Ind. Eng. Chem., 42, 1768, 1950

22. McCabe, B. J. and Eckenfelder, W. W., "Biological Treatment of Sewage and industrial Wastes", Vol. I, Reinhold Pub. Co., N. Y. 1956, p. 215; p. 149.

23. Downing, A. L. and Truesdale, G. A., Jour. of Appl. Chem., 5, 570-581, 1955

24. Truesdale, G. A. and Vandyke, K. G., Water and Waste Treatment Jour., May/June 1958

25. Philpott, J. A. 1952 Ph. D. Thesis, Univ. of London

26. Carpani, R. E. and Roxburgh, J. M. Can. Jour. of Chem. Engr., 36, 2, April 1958

27. Bartholomew, W. H., Karow, E. O., and fat, W. R. Ind. Eng. Chem., 42, 1810, Sept. 1950

28. Cappock, P. D. and Micklejohn, G. T., Trans. Inst. Chem. Engrs., (Br) 29, 75, 1951

29. Haslam, R. T., Hershey, R. L., and Keen, R. H., Ind. Eng. Chem., 16, 1225, 1924

30. Cullen, E. J. and Davidson, J. F., Chem. Eng. Science 6, 2, November 1956

31. Lindland. S. J. and Terjesen, S. J. Chem. Eng. Science 5, 1, February, 1956

32. Eckenfelder, W. W., Lauria, D. and Raymond, L. Sew. and Ind. Wastes

33. Heyrovsky, J., Trans. Faraday Soc., Vol. 19, p. 785. 1924

34. Kolthoff, I. M., and Lingane, J. J., "Polarography" Vol. 1, 2nd Edition, Interscience Publishers, New York, N. Y., 1952

35. Ewing, G. W., "Instrumental Methods of Chemical Analysis", McGraw Hill Book Co., New York, N. Y. 1954;

36. Rand, M. C. and Heukelekian, H., Sew. and Ind. Wastes, 23, 1141, 1951

37. "Standard Methods for the Examination of Water, Sewage and Industrial Wastes," American Public Health Assoc. Inc., New York, N. Y., Tenth Edition (1955)

38. Seaman, W. and Allen, W., Sew. and Ind. Wastes, 22, 912, 1950

39. Lamb, M., Proc. First International Conference on Water Pollution Research, London, 1962

40. McKeown, J. J., and Okun, D. A., Proc. 3rd Biological Waste Treatment Conference, Manhattan College, 1960

41. Eckenfelder, W. W., Proc. A.S.C.E., Jour. S.E.D., July, 1959

APPENDIX I

ANALYTICAL METHODS

Oxygen Analysis by the Polarographic Method

Disagreement has been observed between the Winkler method and the Polarographic method for oxygen in solutions containing known impurities and various industrial waste mixtures. Dissolved oxygen determinations were made using the Pomeroy modification (38) of the Winkler method on solutions containing various concentrations of peptone and on several industrial wastes. These data were compared with results obtained using the polarograph calibrated with one percent potassium chloride solution. At high peptone concentrations the chemical and polarographic methods were not in agreement. Dissolved oxygen determinations made on Kraft mill wastes also showed a wide variation between the chemical and polarographic methods. Similar results were obtained by Rand and Heukelekian (36) with large errors being observed in the dissolved oxygen content of several industrial wastes as measured by the Winkler method. Their results show that the polarographic method permits reasonably accurate determinations of dissolved oxygen even under conditions which render the Winkler method inapplicable.

The Polarographic method of analysis depends on the ability of oxygen to be reduced at a cathode immersed in a test solution. The dropping mercury electrode has proven to be a suitable cathode for this purpose since the metal surface is continually renewed and thus cannot become fouled or poisoned. A saturated calomel electrode serves as the anode.

In 1924, Heyrovsky (33) first reported that oxygen dissolved in electrolyte solutions is reduced at the dropping mercury electrode to produce two waves of equal height. The good development of the diffusion currents and their linear dependence on oxygen concentration, makes possible the accurate polarographic determination of oxygen.

The first wave results from reduction to hydrogen peroxide -

$$O_2 + 2\,H^+ + 2\,e^- \rightarrow H_2O_2 \qquad \text{(acid medium)}$$

$$O_2 + 2H_2O + 2^- \rightarrow H_2O_2 + 2\,OH^- \text{(neutral or alkaline medium)}$$

and the second corresponds to the reduction of the hydrogen peroxide either to water or hydroxide ion depending on the pH:

$$H_2O_2 + 2\,H^+ + 2\,e^- \longrightarrow 2\,H_2O \quad \text{(acid medium)}$$

$$H_2O_2 + 2\,e^- \longrightarrow 2\,OH^- \quad \text{(alkaline medium)}$$

The first oxygen wave displays a very pronounced maximum, but this is easily suppressed by the addition to the solution of a small amount of some organic substance, usually colloidal or of high molecular weight. Gelatin is often satisfactory, though dextrose and various dyes such as methyl red, will sometimes serve. This phenomena is not fully understood although it appears to be related to the physical adsorption of dissolved material on the surface of the mercury.

A small amount of electricity, the residual current, is always observed to flow through the cell even at a potential below that of any reducible matter present. This must be subtracted from the limiting current to give that value which is actually a measure of diffusion of the ions.

The mathematics of polarography was developed by J. Heyrovsky, D. Ilkovic and their co-workers in Czechoslovakia. The Ilkovic equation which resulted has been discussed in considerable detail by Kolthoff and Lingane (34). This equation is as follows:

$$I_d = 605\ n\ CD^{1/2} m^{2/3} t^{1/6}$$

Where I_d is the diffusion current (in microamperes); n is the number of electrons involved in the reduction process taking place at the cathode; C is the concentration of reducible material in solution (in millimoles per liter); D is the coefficient of diffusion of the reducible substance (in sq. cms. per sec.); m is the mass of mercury (in mgms.) flowing through the capillary per second; and t is the time between successive drops (in seconds).

The value of m for any one capillary will remain constant if the hydrostatic pressure on the mercury is kept the same. The drop time t varies not only with the pressure of mercury but also as a function of the applied potential.

Although the temperature does not enter explicitly into the Ilkovic equation, it is nevertheless important, as each factor of the equation (except n) is to some extent temperature dependent. The chief effect is through the temperature coefficient of diffusion constant D. It has been found that the value of the diffusion current I_d increases at the rate of 1 or 2 percent per degree in the vicinity of room temperature.

Under certain conditions the Ilkovic equation fails to describe adequately the factors which determine the diffusion current. The current becomes much larger than predicted and less reproducible if the drop time t becomes less than 3 or 4 sec. The effect is due to the stirring action of the fast falling drops which disturb the diffusion layer.

The diffusion coefficient D varies with the viscosity of the medium, and hence such a variation is found in the diffusion current. If other factors are held constant, the current should be inversely proportional to the square root of the relative viscosity. This relation is found to be valid in the absence of colloidal material, but the proportionality fails when the viscosity is increased through the addition of a hydrophilic colloid.

The diffusion current varies from its normal value if the concentration of supporting electrolyte is less than twenty-five or thirty times that of the reducible material.

Many factors which are difficult to handle in a polarographic analysis can be avoided by making only relative measurements. To do this it is necessary to prepare a standard solution of the desired material and determine its current-voltage curve under the same conditions as the unknown. Then the Ilkovic equation can be applied in the simplified form

$$I_d = KC$$

Apparatus

A manually operated Sargent Polarograph (Model III) was used for oxygen analysis. It provided facilities for applying incrementwise a polarizing potential at the dropping mercury electrode and for measuring the resultant current passing through the electrolysis cell.

The dropping mercury electrode assembly consists of a capillary tube attached to a vertical glass tube in which the mercury height can be regulated to give the proper dropping rate. The mercury is supplied to this tube from a reservoir. The sample solution is contained in a 100 ml beaker into which the dropping mercury electrode and a saturated calomel electrode are inserted when readings are to be taken.

Experimental Procedure

The polarograph is standardized against an air saturated one percent potassium chloride solution. The current vs voltage curve is plotted for this solution to locate the plateau region which determines the applied potential suitable for analysis. While a recommended procedure for oxygen analysis by the polarographic method (36) suggests addition of methyl red as a maximum suppressor, Seaman and Allan (37) reported that with one percent potassium chloride solution no suppressor is necessary.

The galvanometer zero reading for the polarograph is noted and recorded. Using the operating potential as determined from the polarogram plateau, the residual current is obtained by purging a sample with nitrogen for ten minutes or until a constant minimum reading is obtained on the polarograph. The solution is then aerated until saturation is indicated by a constant polarograph reading.

In order to correct for the residual current the following equation is used:

$$D_t = (D_{air} - I) \times c.m. - (D_p - I) \times c.m.$$

where

D_t = net galvanometer reading at temperature t due to dissolved oxygen

D_{air} = galvanometer reading at temperature to for solution containing dissolved oxygen

D_p = galvanometer reading at temperature to due to residual current

I = instrument zero

c.m = current multiplier on instrument galvanometer.

Since the diffusion current varies with temperature it is necessary

to correct to some standard temperature, 20°C in this case. The correcting equation is as follows:

$$D_{20} = D_t \quad 1 + 0.014 (20 - t)$$

where

D_{20} = galvanometer reading at 20°C

D_t = galvanometer reading at t°C

t = temperature at which the determination was made.

The number 0.014 is involved because the oxygen diffusion current changes 1.4 percent for each centigrade degree variation from 20°C.

A calibration factor is computed as $f = \frac{C}{D_{20}}$

where

C = dissolved oxygen concentration in one percent potassium chloride solution at temperature t (in parts per million).

D_{20} = galvanometer reading corrected to 20°C

Once the calibration factor is available the polarograph can be used to determine the dissolved oxygen content of various solutions. An oxygen polarogram for the solution is run to locate the plateau which determines the operating potential. The unknown sample is placed in the cell of the instrument, the predetermined voltage is applied to the electrode and the resulting current noted. The temperature of the sample is taken. The diffusion current noted is then corrected for residual current and temperature in the manner described previously. The concentration of oxygen in parts per million can be obtained by multiplying this corrected current value by the calibration factor.

This method of analysis is valid as long as the diffusion current produced by a unit concentration of dissolved oxygen in the test solution is the same as that produced by the same amount of oxygen in the one percent potassium chloride solution.

Effect of Impurities on the Oxygen Polarogram

Since the polarographic method of analysis presumes the availability of a suitable polarogram for oxygen in all solutions being analyzed, an investigation was undertaken to determine the effect of certain impurities on the polarogram. The material whose solutions were studied from this point of view were peptone, castile soap and sodium stearate.

With water plus one percent potassium chloride two plateaus were observed, corresponding to the limiting conditions for the two electrode reactions for oxygen. These occurred at 0.6 volts and 1.6 volts, agreeing with previously reported values (37). Typical polarograms for

oxygen dissolved in various solutions are shown in Figure A1. When the potassium chloride was replaced by peptone in concentrations of 50 ppm and 500 ppm, some shifting of the plateau regions was noted for the 500 ppm concentration, to 0.8 volts and 2.0 volts. An unsatisfactory polarogram resulted when a peptone concentration of 50 ppm was used. These curves are shown in Figure A2

Since a satisfactory polarogram was obtained with the potassium chloride solution alone and with the 500 ppm peptone solution but not for the 50 ppm solution it would appear that a certain minimum concentration of electrolyte is necessary. Ewing (35) has pointed out that the diffusion current varies from its normal value if the concentration of supporting electrolyte is less than twenty-five or thirty times that of the material being analyzed. Since the solubility of oxygen in water at room temperature is slightly less than 10 ppm, the minimum concentration of supporting electrolyte required would be approximately 250 ppm, well above the 50 ppm concentration in the peptone solution giving the unsatisfactory results. When polarograms were obtained in solutions containing 50 ppm peptone and 500 ppm peptone plus one percent potassium chloride, satisfactory results were obtained.

A similar series of polarograms for dissolved oxygen was determined in castile soap solutions. The results are shown in Figure A3. Here it can be seen that the first plateau region has apparently been suppressed by the action of the soap, although at the higher potentials a plateau region developed. Adding one percent of potassium chloride to the solutions did not improve the polarogram to any great extent when castile soap was present except to shift the plateau regions to lower potential values by decreasing the resistance in the cell.

Comparison of Polarographic and Chemical Methods of Oxygen Analysis

Experimental

Solutions containing 5, 25, 50 and 100 ppm sodium stearate were prepared and oxygen polarograms were determined for each of these solutions under conditions of oxygen saturation. In each case (with the exception of the 5 ppm solution) the first plateau region occurred at a potential of 1.0 volts as compared to a potential of 0.5 volts for a 1% KCl solution. This indicates that 1.0 volt must be used when analyzing for oxygen in solutions of this type.

It was desired to compare the results from the Polarographic method and the Winkler method with published data to determine the relative accuracies of these two methods. The Winkler method (Azide modification) was compared with published data (p. 254, Standard Methods, 10th Edition) by saturating water, 0.5% and 1.0% KCl solutions with oxygen and analyzing by this method. The results are given in Table A1. Results obtained during the summer of 1956 have also been included in Table A1. The accuracy of the Winkler method is the same for both sets of results, being on the average 0.56 ppm or 7.6% too low for the results obtained in 1956. It might be pointed out that the 1956 and 1957 results were obtained by different analysts.

The following procedure was used for making this comparison:

A 200 ml. sample of the solution to be analyzed was placed into each of three glass cylinders having a capacity of 425 ml. each. These three solutions were purged with nitrogen until a minimum polarographic reading was obtained. A sample of distilled water was aerated until a maximum reading (saturation value) was obtained on the polarograph. A 200 ml. portion of this oxygen-saturated water (whose oxygen concentration in parts per million is known from published data) was carefully added to the purged sample of sodium stearate solution, an atmosphere of nitrogen being maintained above the liquid during the addition. When the oxygen saturated water had been added, the cylinder was immediately stoppered and the solution mixed. This procedure was repeated for the other two cylinders. The resulting solutions, whose sodium stearate concentration was half that of the original 200 ml. portion and whose oxygen concentration was half that of the oxygen saturated water, was then analyzed by both the Winkler and the Polarographic methods and compared with the calculated (handbook) values. The Polarographic analysis was carried out at a potential of 0.5 volts (KCl plateau) and 1.0 volts (sodium stearate plateau).

This procedure was repeated using sodium stearate solutions containing 1% KCl solution instead of the distilled water mentioned previously.

The results are given in Table A2

These results show that, in the absence of KCl, a potential of 1.0 volts is necessary if correct results are to be obtained for the sodium stearate solutions. On the other hand, if KCl is present in solution either by itself or with sodium stearate, a potential of 0.5 volts must be used. Even though the 5 ppm sodium stearate solution gives an unsatisfactory oxygen polarogram, the experimental results as reported in Table 4 are not too far from the calculated value since this polarogram has a current value at 1.0 volt corresponding to the plateau current of the other sodium stearate curves.

On the average, the chemical methods give a result about 7.5% below the published value, agreeing with the results noted previously and reported in Table A1. The results obtained by the Polarographic method in general agree quite closely with those obtained by the Winkler method. The factor used in calculating the oxygen concentration in the Polarographic method was determined using the oxygen saturation value given in Standard Methods, 10th Edition.

The polarographic method of oxygen analysis was found to be applicable for solutions of sodium stearate up to concentrations of 100 parts per million provided certain experimental conditions are met. For solutions of sodium stearate in the concentration range 25 ppm to 100 ppm, satisfactory results were obtained even in the absence of added electrolyte provided the applied potential was 1.0 volt. In the absence of KCl, incorrect values result if 0.5 volts is used. With the 5 ppm sodium stearate solution, satisfactory results are obtained if 1% KCl is added and a potential of 0.5 volts applied.

Surface Tension and Viscosity

The surface tensions of the solutions under investigation were determined by the use of the DuNuoy tensiometer. The Ostwald viscosimeter was used for viscosity determinations.

It was noted that when the surface tension for solutions of sodium stearate were being determined that check results were difficult to obtain. This was attributed to a change in the characteristics of the solution with time. In view of this, it is recommended that when an attempt is made to determine the effect of surface tension on oxygen transfer rate in the aeration column a series of surface tension values be obtained at the same time as the oxygen analyses are being made. Otherwise no valid correlation of oxygen transfer rate with surface tension will be possible. The surface tension of the test solutions employed is shown in Table A3

TABLE A1

COMPARISON OF WINKLER OXYGEN RESULTS WITH PUBLISHED* VALUES

Date	Solution	Temp. °C	ppm O_2 (Winkler)	ppm O_2 (Standard Methods)	Difference Actual (ppm)	Difference %
6/28/57	H_2O	31.0	6.95	7.40	0.45	6.1
7/ 1/57	H_2O	30.0	6.99	7.53	0.54	7.2
6/28/57	5,000 ppm KCl	31.0	6.70	7.20	0.60	8.3
7/ 1/57	" " "	27.8	6.80	7.66	0.86	11.3
6/28/57	10,000 ppm KCl	31.6	6.75	6.90	0.15	2.2
7/ 1/57	" " "	28.6	6.65	7.35	0.70	9.5
7/ 3/57	" " "	28.0	6.80	7.43	0.63	8.5
				Average	0.56	7.6%
7/21/56	10,000 ppm KCl	25.0	7.95	7.86	-0.09	-1.1
7/25/56	" " "	25.0	7.07	7.86	0.79	10.0
7/26/56	" " "	25.0	7.25	7.86	0.61	7.8
8/ 1/56	" " "	25.0	7.17	7.86	0.69	8.8
8/ 2/56	" " "	25.0	7.30	7.86	0.44	5.6
8/ 3/56	" " "	25.0	7.24	7.86	0.62	7.9
				Average	0.54	6.9%

* Standard Methods for the Examination of Water, Sewage and Industrial Wastes, 10th Edition, 1955, p. 254.

TABLE A2

COMPARISON OF WINKLER AND POLAROGRAPHIC RESULTS WITH PUBLISHED DATA

Date	Solution Tested	Calc. Value*	Sample #1 Winkler	Sample #1 Pomeroy	Sample #1 Polar. 0.5v	Sample #1 Polar. 1.0v	Sample #2 Winkler	Sample #2 Pomeroy	Sample #2 0.5 v	Sample #2 1.0v	Sample #3 Winkler	Sample #3 Pomeroy	Sample #3 Polar. 0.5v	Sample #3 Polar. 1.0v
7/ 5/57	10,000 ppm KCl	3.60	3.68	-	3.72	6.43	3.72	-	3.63	6.20	3.34	-	3.02	5.42
7/5/57	50 ppm Na Stearate	3.75	-	3.72	3.01	4.00	3.48	-	2.47	3.31	3.39	-	2.31	3.01
7/8/57	100 ppm Na Stearate	3.78	-	4.06	2.62	3.50	2.96	-	2.42	3.23	3.34	-	2.28	2.96
7/8/57	5 ppm Na Stearate	3.78	-	3.97	1.40	3.15	3.39	-	1.20	3.09	3.39	-	1.00	2.82
7/8/57	25 ppm Na Stearate	3.77	-	3.97	2.98	3.82	3.48	-	2.48	3.76	3.34	-	1.93	3.01
7/9/57	100 ppm Na Stearate +1% KCl	3.70	-	2.52	2.50	4.22	3.00	-	2.36	4.10	3.10	-	2.32	4.14
7/9/57	5 ppm Na Stearate +1% KCl	3.70	-	3.68	3.42	5.95	3.48	-	3.24	5.79	3.38	-	2.79	5.00
7/9/57	25 ppm Na Stearate +1% KCl	3.70	-	3.48	2.82	4.90	3.48	-	2.95	5.09	3.20	-	2.34	4.36

Note: The polarographic data for 7/9/57 should be viewed as only an approximation since difficulty was encountered with the Polarograph on this date.

* These values have been corrected to the pressure of the experimentally determined results.

TABLE A3

SURFACE TENSION OF TEST SOLUTIONS

Solution	Concentration (ppm)	(° C)	Surface Tension (Dynes/cm)
Peptone	0	23.0	71.7
	25	23.0	71.7
	50	23.0	71.7
	100	24.0	71.0
	250	23.5	69.0
	500	24.0	67.5
	1000	24.0	65.1
	2500	24.0	63.1
	5000	25.0	60.0
Peptone	0	24.0	71.4
	50	24.0	71.2
	100	25.0	70.5
	250	25.0	68.8
	1000	24.5	65.0
	1500	25.0	64.3
	2500	25.0	61.3
	4000	25.0	60.0
	5000	25.0	59.5
Peptone	0	24.0	71.9
	1000	25.5	69.4
	2000	26.0	67.7
	3000	26.0	62.3
	4000	25.0	61.8
	5000	24.5	60.5
Sodium Stearate (surface tension determined 1 hr. after solution was prepared)	0	30.2	72.0
	5	30.2	56.0
	10	30.6	50.0
	25	30.6	39.5
	50	31.0	33.4
Sodium Stearate (surface tension determined 3 hrs. after solution was prepared)	0	30.2	72.0
	5	30.2	66.2
	10	30.0	60.0
	25	30.0	44.5
	50	30.0	39.0
Sodium Lauryl -Sulfate	0	27.6	72.0
	5	30.0	62.0
	10	30.0	56.0
	25	30.0	51.0
	50	30.0	45.0
	100	30.0	43.0
	200	30.0	39.6

APPENDIX II - TABLE 1

OXYGEN TRANSFER CHARACTERISTICS OF NYLON SPINNERETTE IN WATER

Temp. °C	G_s cc/min.	K_La 1/hrs.	d_B cm.	Veloc. cm/sec.	K_L cm/hr.
21.5	66	4.85	0.151	31.10	143.9
21	65	5.28			159
22	115	9.70	0.163	33.90	194
21.5	115	8.54			171
22	115	8.45			169
22	134	11.48	0.353	33.90	214
22	125	10.70	0.177		214
22	171	12.10	0.182	32.10	172
22	171	14.5			206
22	171	14.9			212
25.0	110.0	27.6	.165	34.7	298
25.0	114.0	28.4	.165	34.7	296
25.0	122.0	28.8	.165	34.7	282
30	36.7	10.0	.133	26.9	200
30	36.7	10.2	.133	26.9	206
26.5	126.8	16.5	.142	28.5	95.8
26.5	126.8	22.4	.142	28.5	131.8
26.5	126.8	19.7	.142	28.5	116.1
26.0	126.5	11.1	.142	28.5	64.5
26.0	126.5	15.7	.142	28.5	91.5
27.0	127.2	18.5	.142	32.2	120.6
27.0	131.4	18.2	.142	32.2	115.0
27.0	107.9	17.0	.142	32.2	131.0
23.5	116.3	18.3	.162	18.3	135.3
23.0	117.7	18.8	.162	29.3	138.0
23.0	117.7	18.6	.162	29.3	136.0
20.0	40.0	11.0	.127	33.9	246.
20.0	40.0	10.2	.127	33.9	228.
18.0	37.0	6.14	.144	20.2	113.
20.0	37.0	7.6	.148	21.9	156.
20.0	39.9	8.45	.125	30.4	171.
20.0	39.9	8.25	.125	30.4	167.
20.0	39.9	8.43	.125	30.4	171.
23.0	37.0	8.34	.137	22.0	159.
21.0	37.0	6.86	.133	21.4	124.
20.0	42.0	9.1	.152	21.3	166.
20.0	80.0	15.5	.155	19.2	136.
20.0	118.0	16.9	.139	20.1	95.
20.0	168.0	21.4	.152	21.0	95.
19.5	40.0	5.77	.135	21.2	98.

APPENDIX II - TABLE 1 Cont.

OXYGEN TRANSFER CHARACTERISTICS OF NYLON SPINNERETTE IN WATER

Temp. ^oC	G_s cc/min.	K_La 1/hrs.	d_B cm.	Veloc. cm/sec.	K_L cm/hr.
21.0	10.0	1.83	.078	16.9	57.
21.0	60.0	5.92	.122	20.4	59.4
21.0	120.0	11.9	.119	20.6	57.
21.0	192.0	15.6	.127	20.6	51.3
24.0	73.5	15.35	.179	27.8	243.
22.5	88.9	9.31	.242	30.0	178.
24.0	88.0	14.30	.264	34.0	342.
24.0	91.0	15.0	.185	33.9	240.
23.5	94.7	12.2	.206	28.2	175.
22.5	98.0	10.8	.190	28.0	138.
28.0	120.2	23.5	.146	29.8	199.
24.0	108.8	31.2	.172	31.8	368.
23.5	151.0	18.4	.232	27.8	184.
24.0	151.0	24.75	.205	30.5	240.
24.5	191.5	17.7	.331	37.6	268.
22.0	196.0	15.1	.270	27.5	134.
21.0	72.5	11.1	.157	29.4	128.
22.0	71.	11.7	.157	29.4	134.
22.0	112.0	18.3	.179	28.6	151.
21.5	112.0	16.5	.179	28.6	136.
21.5	135.	21.2	.172	30.4	149.
21.0	142.	20.0	.172	30.4	133.
20.5	160.	21.2	.176	27.5	116.
20.5	160.	22.5	.176	27.5	123.
20.5	160.	23.6	.176	27.5	129.
20.5	196.	24.4	.169	26.8	103.
21.	187.	28.8	.169	26.8	127.
27.5	112.	24.5	.147	34.6	231.
27.5	112.	21.2	.147	34.6	200.
27.5	112.	25.4	.147	34.6	242.
27.0	120.	24.5	.158	39.0	261.
19.0	115.5	17.65	.171	29.8	130.
19.5	109.5	17.8	.171	29.8	138.
20.0	109.5	19.0	.171	29.8	148.

APPENDIX II - TABLE 2

EFFECT OF LIQUID SUBMERGENCE DEPTH
ON OXYGEN TRANSFER CAPACITY

Water Depth cm.	Temp. ^oC	G_s cc/min.	K_La l/hrs.	d_B cm.	V_B cm/sec	K_L cm/hr
			SERIES 1			
120	27.5	112	10.6			100
120	27.5	112	9.07			86
120	27.5	112	11.0	.147	34.6	105
95	27.0	112	10.1			103
95	26.5	121	10.1	.146	37.4	94
70	26.5	113	10.4			103
70	26.5	116	10.5	.148	36.8	102
45	26.5	106	11.65			128
45	26.5	104	13.2	.152	37.4	145
45	26.5	97	12.3			148
			SERIES 2			
120	27	120	10.6	.158	39.0	113
95	27	116	10.6	.161	37.8	115
70	27	111	10.9	.167	37.8	128
45	27	104	10.1	.152	39.2	120
			SERIES 3			
120	19	115.5	7.33	.171	29.8	130
120	19.5	109.5	7.37			138
120	20	109.5	7.90			148
95	20.5	109.7	8.97	.163	34.3	185
95	20.5	109.7	8.18			168
95	21	109.4	8.42			173
70	22	107.2	8.47	.160	32.0	162
70	21.5	101.8	8.58			173
70	22	101.0	9.9			202
45	22	92.6	8.65	.152	31.9	180
45	22	96.	9.80			196
45	22	96	8.85			177

APPENDIX II - TABLE 3
EFFECT OF TEMPERATURE ON OXYGEN TRANSFER IN WATER

Temp °C	Gs cc/min.	K_La 1/hrs.	d_B cm	V_B cm/sec	K_L 1/m
			SERIES 1		
10	22.5	2.49	.136	26.7	191
10	22.5	2.60			200
10	22.5	2.49			191
20	21.8	3.16	0.157	33.2	358
20	21.8	3.08			350
30	21.4	3.82	0.127	35.8	386
30	22.0	3.83			374
40	20.4	5.24	0.140	32.6	555
40	21.3	5.10			520
			SERIES 2		
10	49.3	3.55	0.142	33.7	165
10	49.3	3.85			179
20	48.6	4.59	0.175	30.2	237
20	48.6	4.64			246
30	50	6.97	0.138	33.8	308
30	48.0	6.10	0.192	31.4	364
30	48.0	6.53	0.192	31.4	389
40	46.6	7.59	0.158	34.5	423
40	46.6	7.01	0.158	34.5	390
40	46.6	7.05	0.158	34.5	394
			SERIES 3		
10	41.4	2.94	0.204	33.1	229
10	41.4	3.05	0.204	33.1	236
10	40.6	2.79	0.194	37.0	234
10	40.6	3.05	0.194	37.0	257
10	40.6	3.07	0.194	37.0	257
20	39.8	4.01	0.200	38.4	370
20	39.8	3.51	0.200	38.4	322
20	39.2	3.53	0.200	38.4	329
20	39.3	4.23	0.186	35.4	338
20	40.0	4.23	0.186	35.4	332
30	37.8	4.46	0.197	33.5	370
30	37.8	4.85	0.197	33.5	403
30	37.8	4.51	0.197	33.5	376
30	37.8	5.04	0.182	36.4	421
30	40.4	5.25	0.172	39.1	416
30	37.9	4.70	0.172	39.1	322
30	37.9	4.90	0.172	39.1	330
40	36.7	5.15	0.198	31.6	419
40	36.7	4.34	0.198	31.6	352
40	36.7	4.62	0.198	31.6	376
40	36.7	4.41	0.198	31.6	358

APPENDIX II - TABLE 4

EFFECT OF TEMPERATURE ON OXYGEN TRANSFER IN A 50 mg/l SOLUTION OF HEPTANOIC ACID

Temp. °C	G_s cc/min.	K_La 1/hrs.	d_B cm.	Vel. cm/sec	K_La cm/hr
		SERIES 1			
8	121.5	4.11	.140	21.1	96.
8	124.4	3.44			79.
8	127.1	2.40			53.5
9	126.2	3.62			81.5
		SERIES 2			
9	113.5	3.27	.135	20.5	77.
9	107.2	3.23			80.5
10	107.1	2.93			73.
21	109.0	4.24	.107	22.0	88.
21	106.7	4.66			100.
21	109.0	3.93			81.5
32	107.1	4.70	.128	20.2	109.
30	105.7	5.92			139.
30	101.0	4.80			118.
		SERIES 3			
31	112.1	6.20	.136	21.6	150.
30	109.1	5.26			137.
29.5	106.5	5.87			156.
30	105.8	4.70			126.
31	112.0	4.67			119.
19	119.0	4.02	.140	19.4	88.
20.5	113.0	3.6			83.5
21	109.0	4.03			97.
10	116.8	2.55	.138	17.9	52.
10	120.0	3.15			63.
		SERIES 4			
40	46.4	5.57			144.
40	46.4	6.14	.118	21.175	159.
40	46.4	5.65			146.
30	47.8	4.55			109.
30	47.8	5.00	.1196	20.06	119.5
30	47.8	5.25			125.5
20	49.5	3.60			94.5
20	49.5	4.02	.1281	21.23	106.5
20	49.5	3.91			102.5
10	51.4	3.19	.1338	20.275	81.
10	51.4	3.19			81.

APPENDIX II - TABLE 5
OXYGEN TRANSFER CHARACTERISTICS IN N-HEPTANOIC ACID
SPINNERETTE - 20 - 0.035 m m holes

Conc. mg/l	Temp. ^oC	G_s cc/mm	K_La 1/hrs.	d_B cm.	V_B cm/sec	K_L cm/hr.
10	26	56.7	10.8	.178	29.3	232
10	26.	12.0	15.5	.175	31.6	168
10	26.5	21.0	31.0	.227	32.1	252
50	26.	56.7	8.25	.128	21.9	95.5
50	26.	12.0	16.85	.144	22.7	107.5
50	26.	23.3	35.6	.179	21.5	139.0
100	26.5	57.0	7.30	.137	21.7	89.0
100	26.	12.3	16.40	.144	25.0	112.3
100	26.	23.0	26.0	.132	25.6	89.5
500	24.	55.5	5.57	.139	21.6	71.5

APPENDIX II - TABLE 6

OXYGEN TRANSFER CHARACTERISTICS IN CAPROIC ACID SPINNERETTE - 10 HOLES @ 0.05 m m DIAMETER

Conc. mg/l	Temp. ^{o}C	G_s cc/min.	K_La l/hrs.	d_B cm.	Veloc. cm/sec	K_L cm/hr
			SERIES 1			
0	22	103	8.76	0.147	33.9	176.
0	23	105	8.23			162.
250	22.5	105	5.54	0.138	23.8	72.0
250	22.5	105	5.90			76.7
100	22	105	6.96	0.130	22.6	80.7
100	22.5	105	9.37			169.0
100	23.5	106	11.0			126.5
			SERIES 2			
0	27.0	127.2	8.040	.142	32.2	120.6
0	27.0	131.4	7.92			115.0
0	27.0	107.9	7.38			130.9
10	26.5	114.7	9.68	.149	32.4	162.0
10	26.5	114.7	10.38			174.0
10	26.5	111.0	8.80			152.1
25	26.0	110.8	8.95	.146	25.8	128.5
25	25.5	120.5	11.50			150.3
25	25.5	114.2	10.25			140.9
			SERIES 3			
0	23.5	116.3	7.93	.162	29.3	135.3
0	23.0	117.7	8.16			138.0
0	23.0	117.7	8.06			136.1
10	23.0	117.7	10.40	.146	30.0	162.0
10	23.0	122.2	10.65			159.4
10	23.0	124.7	10.00			147.1
25	23.0	127.4	11.55	.144	25.5	138.6
25	23.0	129.7	11.05			130.8
50	23.0	127.4	9.23	.138	22.0	91.7
50	23.0	127.4	9.45			93.9
100	25.0	123.3	4.89	.138	22.4	51.2
100	24.5	123.2	6.72			70.3
250	24.0	123.1	5.56	.140	22.4	59.1
250	23.5	130.2	6.15			61.9
			SERIES 4			
0	30	36.7	4.31	.133	26.9	201
0	30	36.7	4.44			207
10	30	40.2	5.10	.127	23.96	185
10	30	37.9	5.25			201
25	30	36.7	4.43	.117	21.72	147
25	30	36.7	4.97			164
25	30	36.7	4.84			161

APPENDIX II - TABLE 6 Cont.

OXYGEN TRANSFER CHARACTERISTICS IN CAPROIC ACID
SPINNERETTE - 10 HOLES @ 0.05 m m DIAMETER

Conc. mg/l	Temp. ^oC	G_s cc/min.	K_La 1/hrs.	d_B cm.	Veloc. cm/sec.	K_L cm/hr
			SERIES 5			
0	25	110	12.0			129
0	25	114	12.3	.165	34.7	128
0	25	122	12.5			122
10	25	110	7.75	.166	35.6	86
10	25	116	8.23			86.5
25	25	124	10.3			100
25	25	116	8.88	.164	36.0	93
25	25	115	8.92			95
50	26	110	10.7			117
50	26	118	11.8	.159	36.7	120
50	26	116	10.6			110
100	26	108	12.9			129
100	26	112	12.5	.146	36.05	122
250	26	112	13.2			118
250	26	112	11.5	.142	32.1	110
250	26.5	115	13.5			118

APPENDIX II - TABLE 7
OXYGEN TRANSFER CHARACTERISTICS IN N-CAPROIC ACID
SPINNERETTE - 20 HOLES @ 0.035 mm DIAMETER

Conc. mg/l	Temp. ^oC	G_s cc/mm	K_La 1/hrs.	d_B cm.	V_B cm/sec.	K_L cm/hr.
10	28	54.2	11.5			
10	27	115.2	26.2	.135	31.4	225.
10	27	195.0	25.4	.142	32.1	140.
50	28	53.8	7.8			
50	28	116.	18.25	.102	23.9	89.5
50	28	195.5	25.8	.091	22.6	61.5
100	28	56.0	5.3			
100	27	114.3	23.1	.119	20.4	114.
100	28	214.0	38.8	.102		
500	28	54.0	5.7			
500	28	114.5	18.5	.090	25.4	86.4
500	28	219.0	23.2			
1000	29	62.0	8.75	.081	17.8	47.6
1000	29	126.5	15.82	.091	24.6	65.4
1000	29	218.0	53.0	.077		
2000	28		31.0			

APPENDIX II - TABLE 8

OXYGEN TRANSFER CHARACTERISTICS IN OCTANOIC ACID
SPINNERETTE - 10 HOLES - 0.05 m m Diameter

Conc. mg/l	Temp. ^{o}C	G_s cc/min.	K_La 1/hrs.	d_B cm.	Veloc. cm/sec.	K_L cm/hr
			SERIES 1			
10	20.5	115	8.20	0.142	22.9	96.5
10	21.5	109	9.0			112
20	23.5	115	7.20	0.151	22.2	87.5
20	23.5	115	7.78			94.5
			SERIES 2			
0	21.5	112	7.27	0.180	32.4	158
0	21.5	112	7.68			165
10	24.5	108	10.1	0.144	22.9	129
10	24	110	8.4			105
10	24	113	9.0			110
25	24	113	6.22	0.142	25.15	82
25	24	113	6.32			83.4
50	23.5	117	5.68	0.139	22.8	64
50	24	115	5.03			57.5
50	24	115	4.13			47.1
100	24	110	4.02	0.139	23.3	49.2
100	24	110	4.25			52.1
0	24.5	113	8.71	0.163	33.7	177

APPENDIX II - TABLE 8 Cont.

OXYGEN TRANSFER CHARACTERISTICS IN OCTANOIC ACID
SPINNERETTE - 10 HOLES - 0.05 m m DIAMETER

Conc. mg/l	Temp. ^oC	G_s cc/min.	K_La 1/hrs.	d_B cm.	Veloc. cm/sec.	K_L cm/hr
			SERIES 3			
0	20	40.0	4.76	.127	33.90	245.0
0	20	40.0	4.43			226.0
10	20	40.0	3.66	.121	18.35	96.6
10	20	35.9	3.32	.122	19.90	107.0
10	20	35.9	2.78			89.5
10	20	37.1	3.34			104.2
12.5	20	37.1	3.22	.132	25.75	141.2
25	20	37.1	2.31	.125	21.65	80.2
25	20	39.4	2.20			71.7
50	20	38.8	2.32	.115	19.60	64.0
50	20	39.4	2.35			64.2
50	20	39.4	2.27			61.8
50	20	38.8	2.06			57.0
100	20	38.0	2.01	.114	19.75	56.8
100	20	35.9	1.84			55.0
100	20	35.9	1.98			59.3
250	20	35.9	2.01	.109	19.85	57.8
250	22	35.45	2.11			61.1
250	24	35.8	2.26			62.5

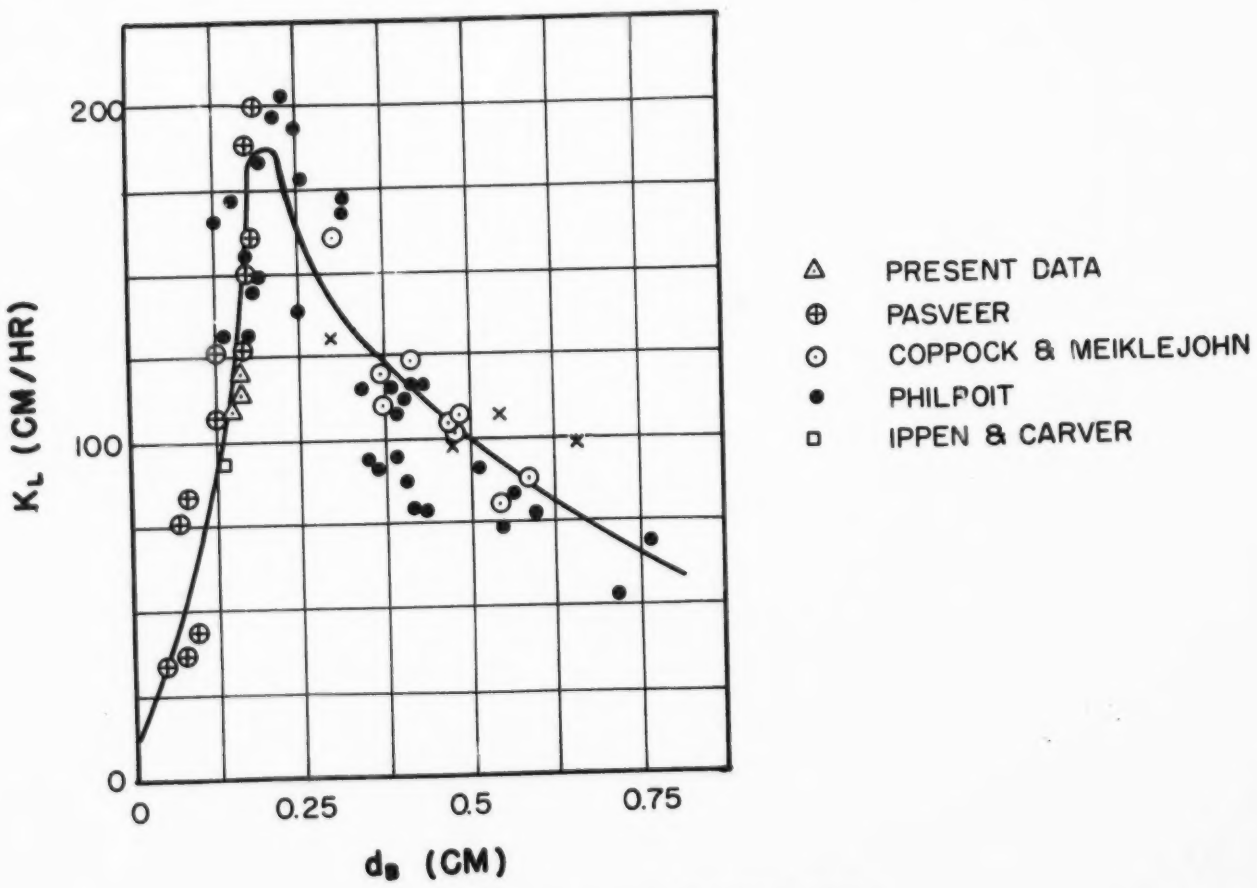

Figure 1 - Relation Between Liquid Film Coefficient and Bubble Diameter

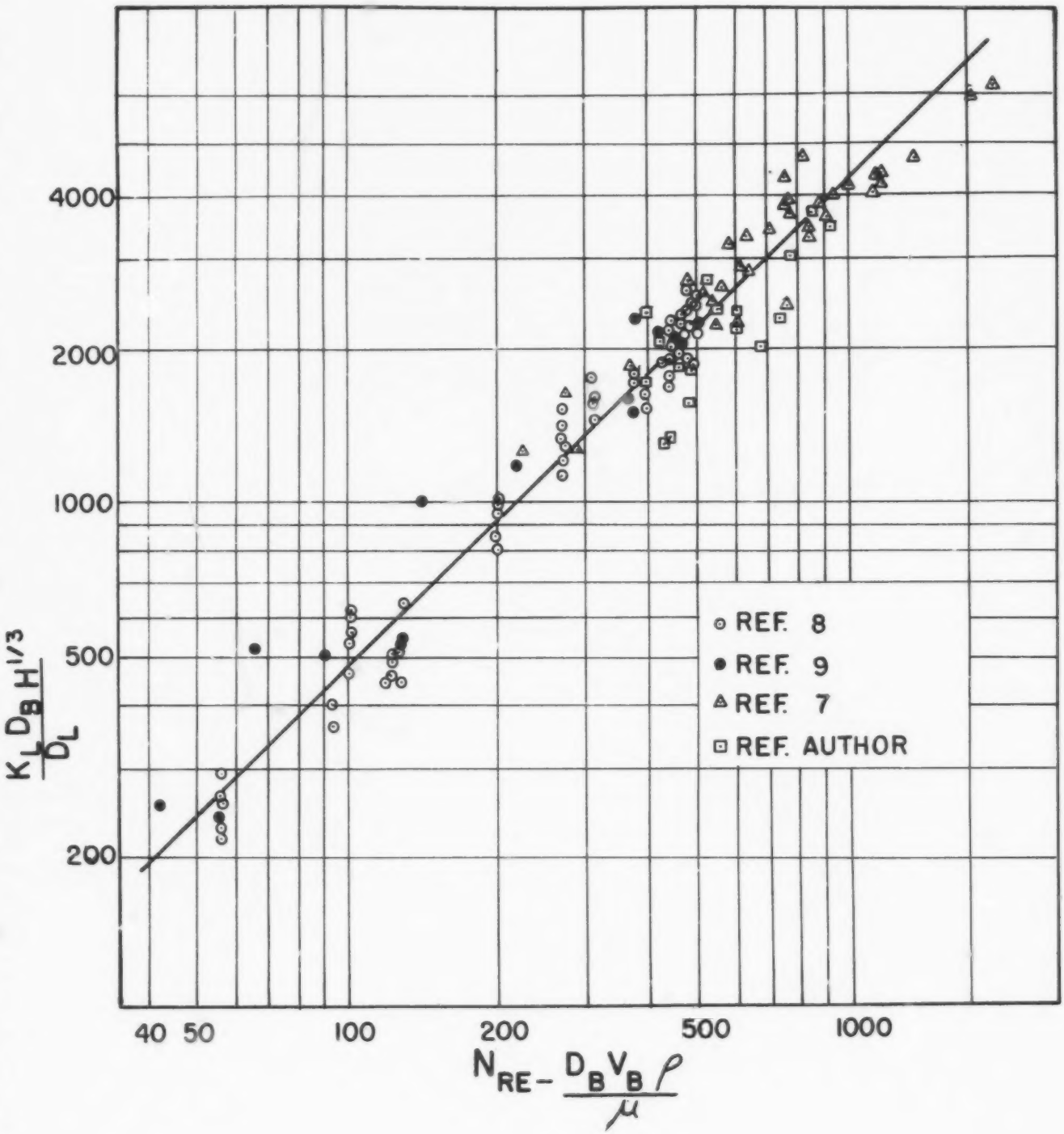

Figure 2 - Correlation of Bubble Aeration Data

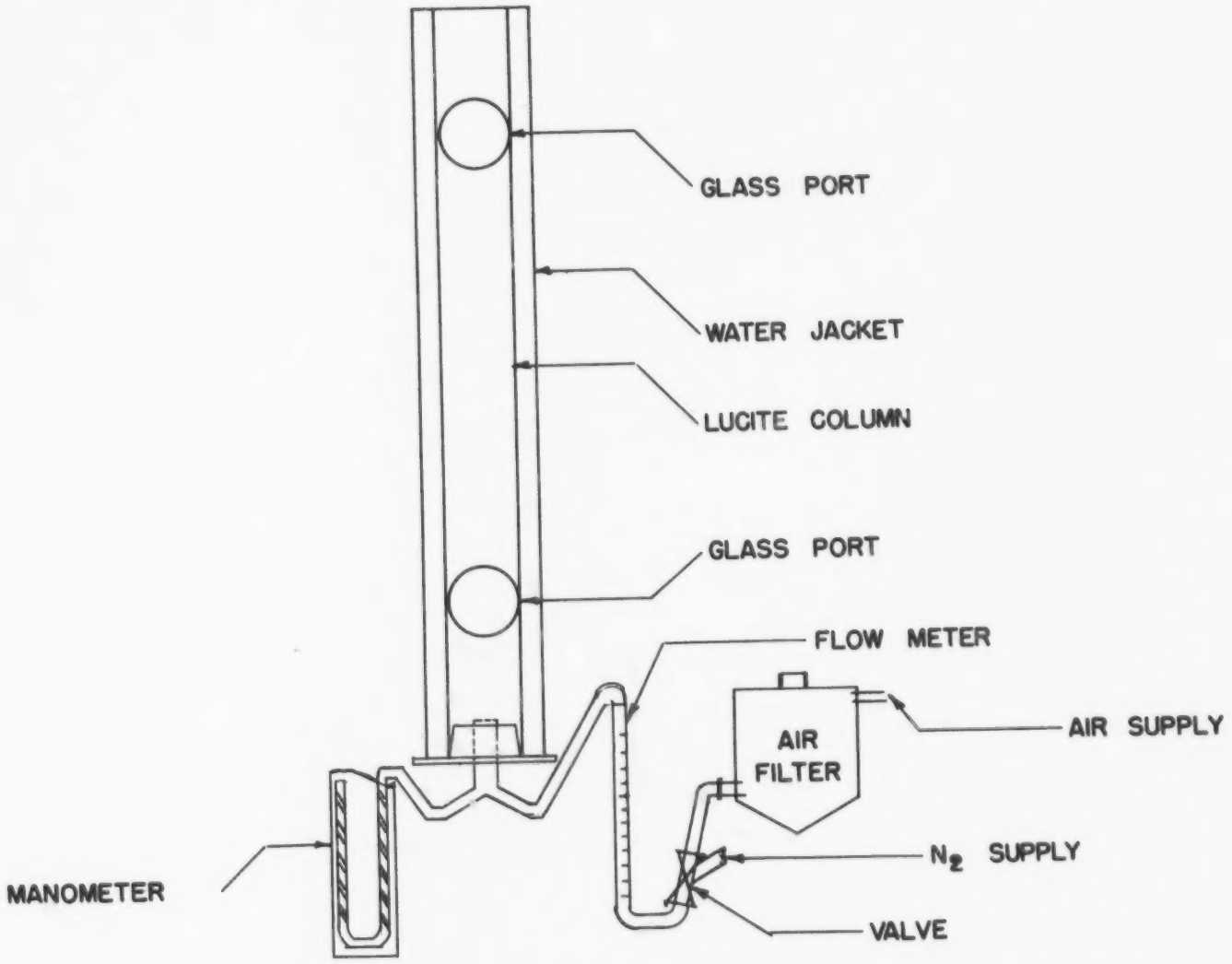

Figure 3 - Experimental Apparatus

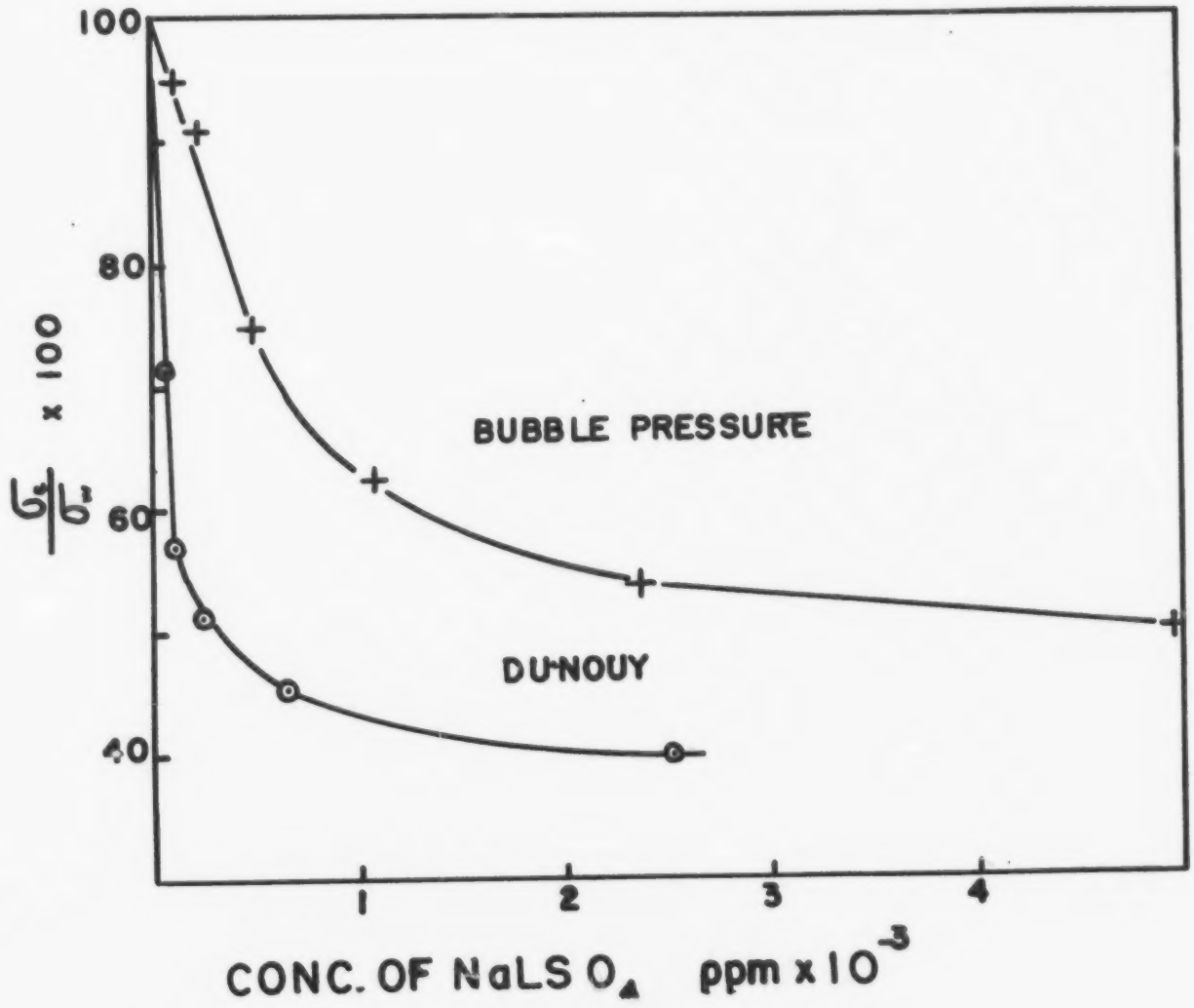

Fig. 4 Surface Tension of Sodium Lauryl Sulfate

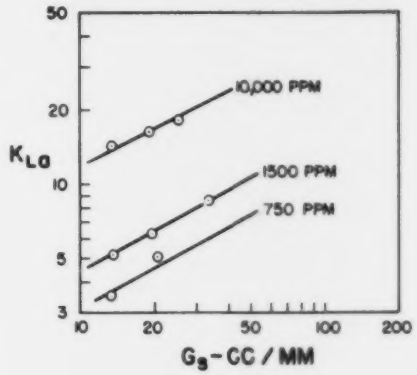

Figure 5 - Relation Between K_La and Air Flow For Solutions of Various Concentrations of Peptone - Aloxite Stone Diffusor

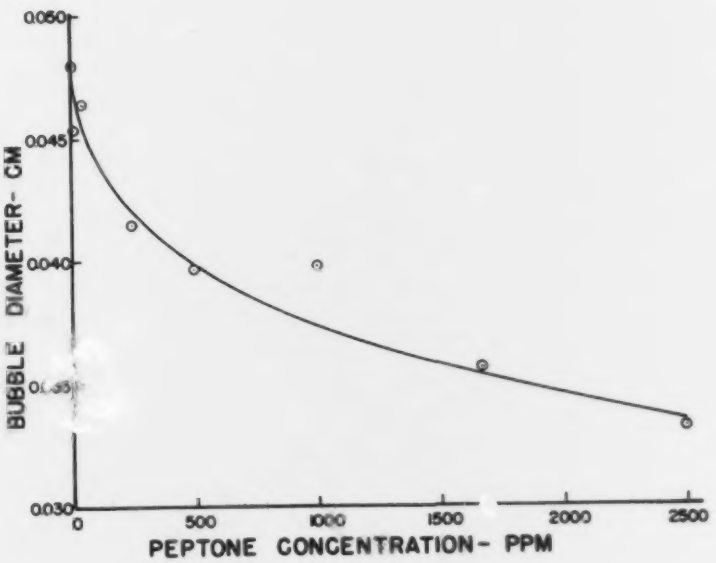

Fig. 6 Variation of Bubble Diameter with Peptone Concentration

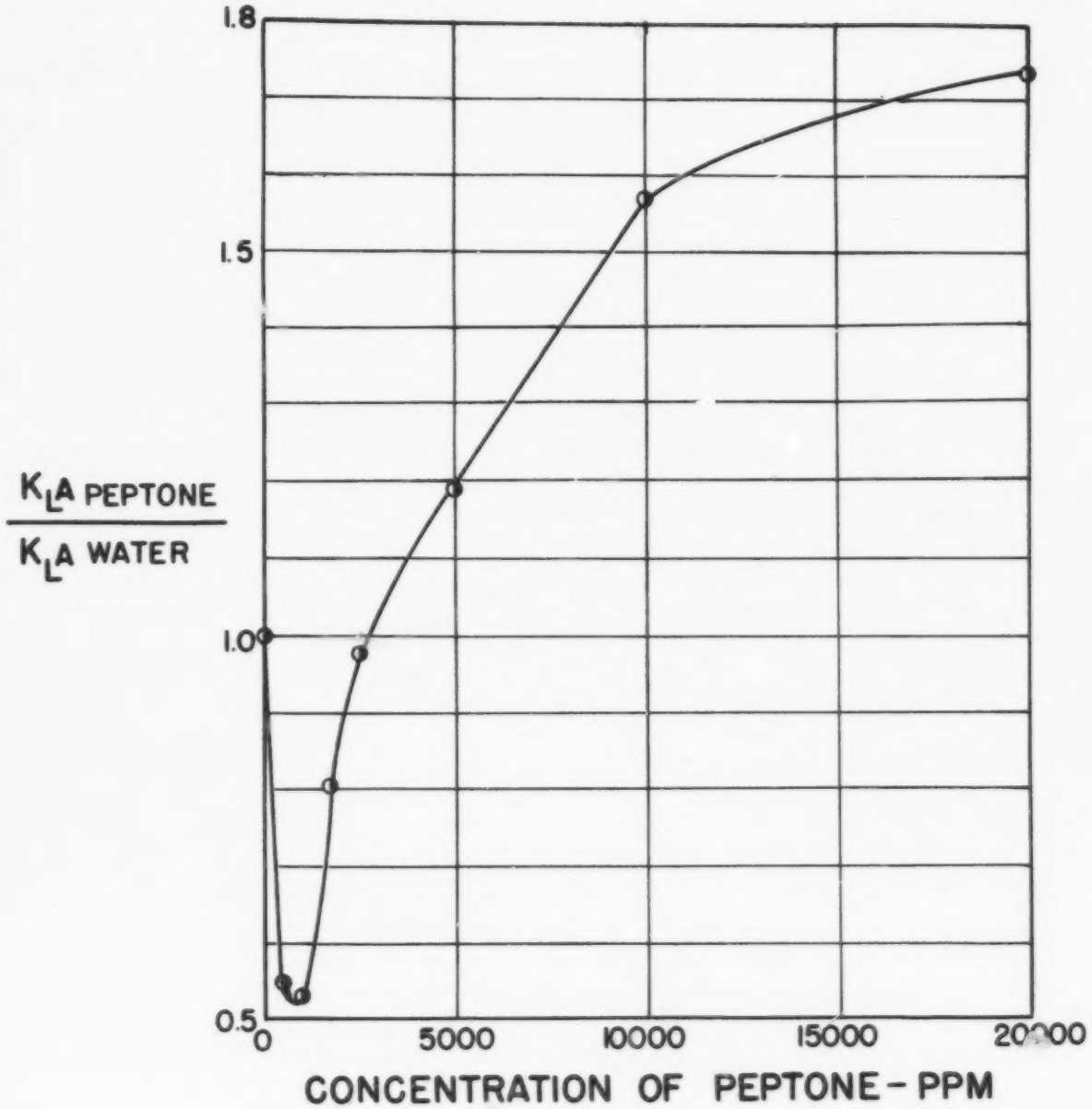

Figure 7 - Variation of the Transfer Ratio, Alpha, Concentration of Peptone Aloxite Stone Diffusor

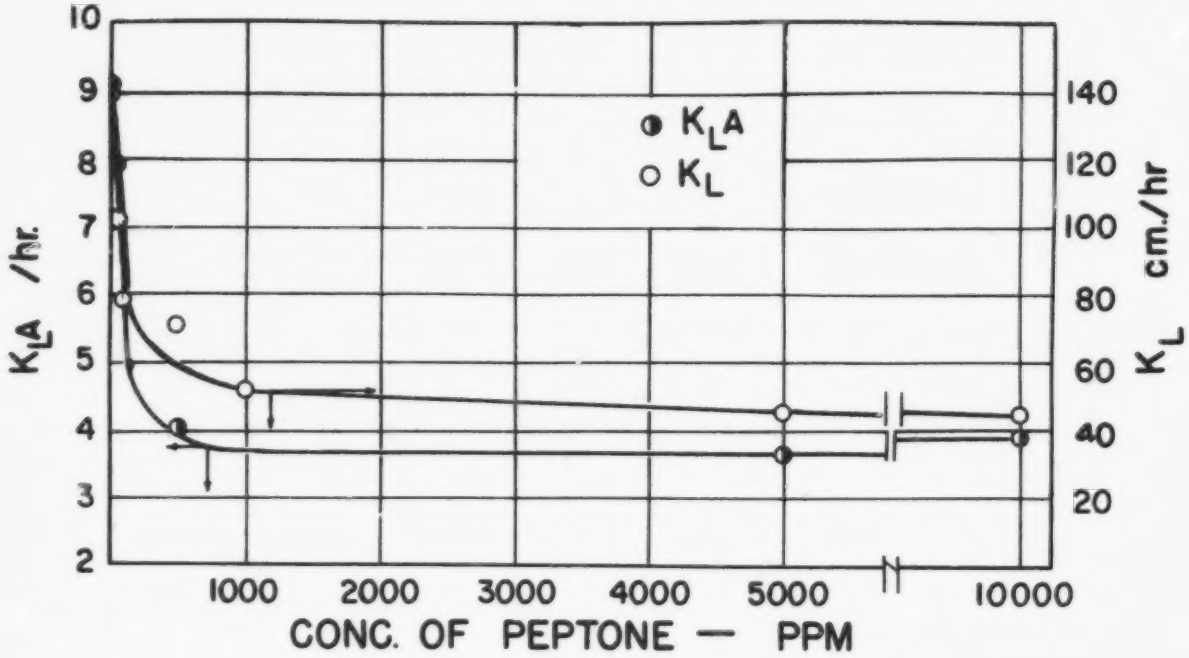

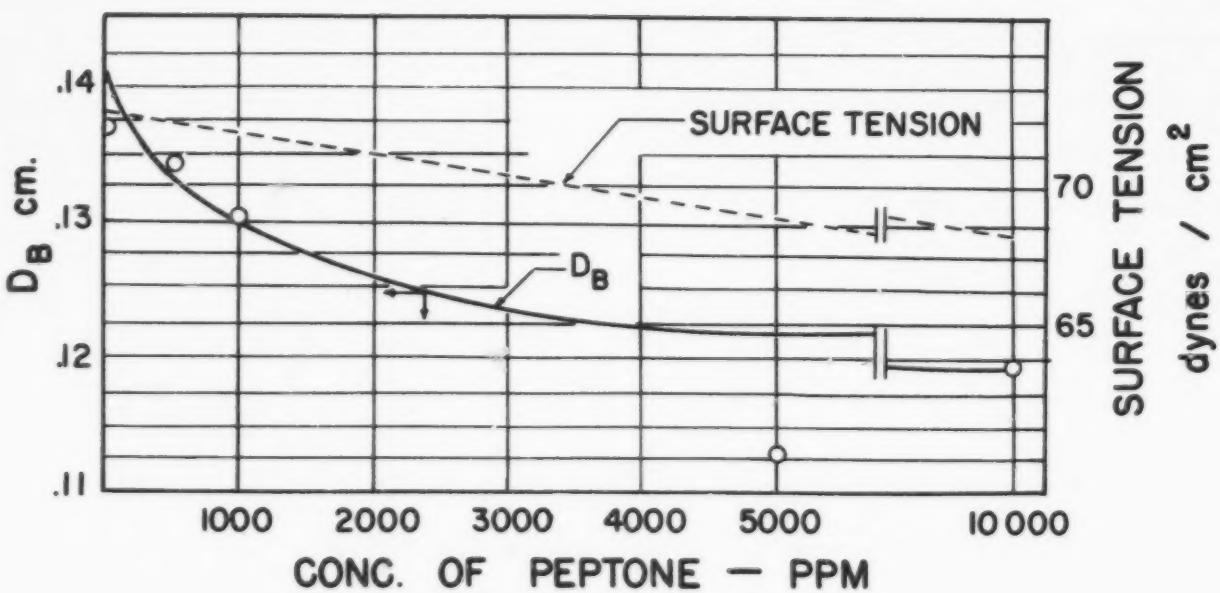

Figure 8 - Oxygen Transfer in Solutions of Various Concentrations of Peptone
Nylon Spinnerette

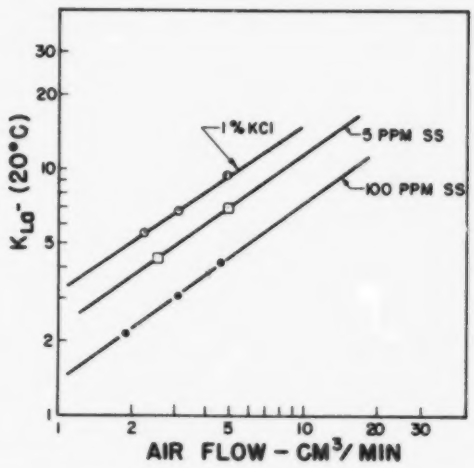

Figure 9 - Relation Between K_La and Air Flow for Solutions of Various Concentrations of Sodium Stearate

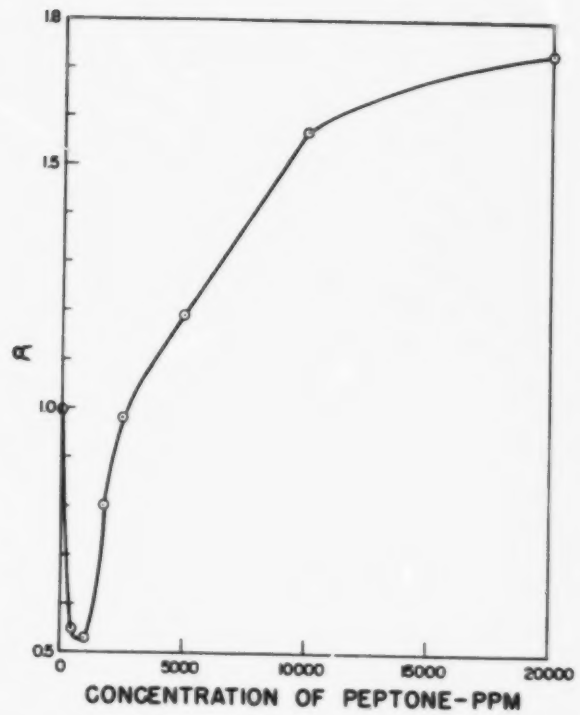

Figure 10 - Variation of the Transfer Ratio, Alpha, With Concentration of Sodium Stearate - Aloxite Stone Diffusor

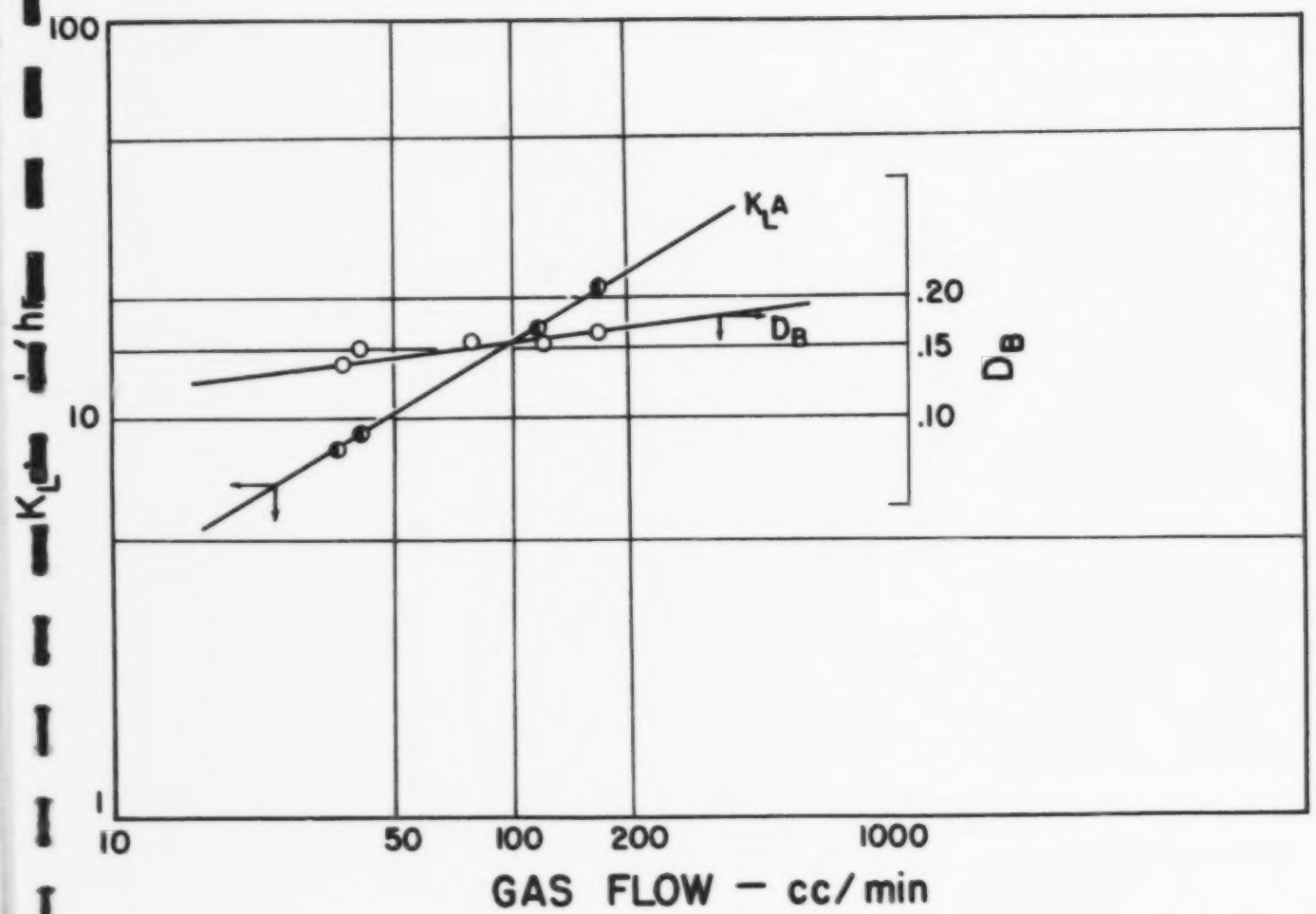

Figure 11 - Relationship Between K_La - d_B and Air Flow for the 0.035 mm Spinnerette

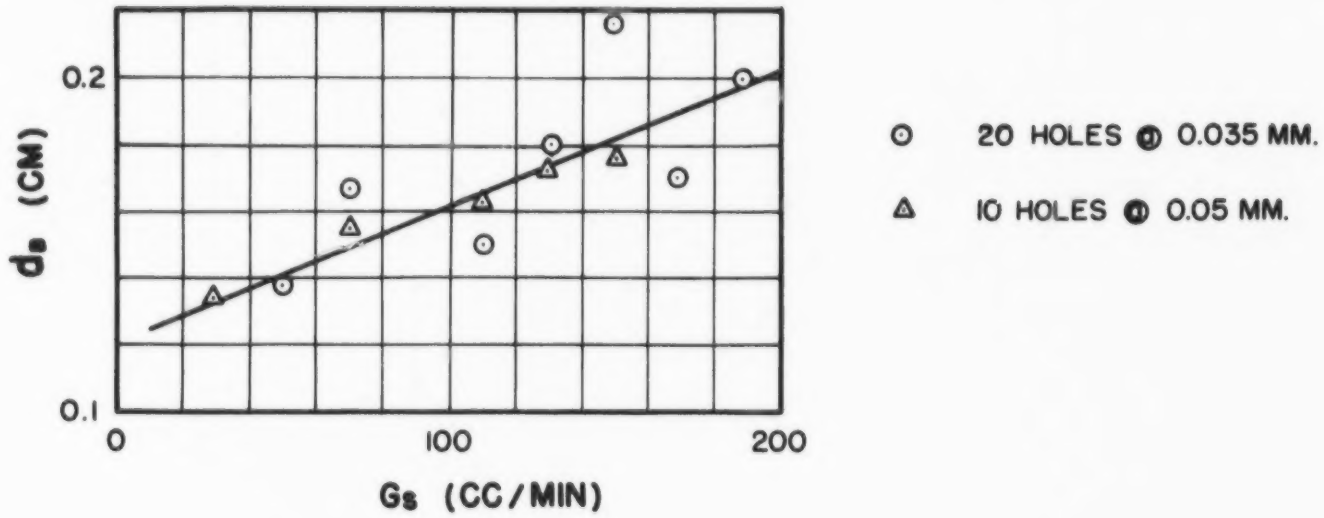

Figure 12 - Relationship Between G_s and d_B for the Nylon Spinnerettes

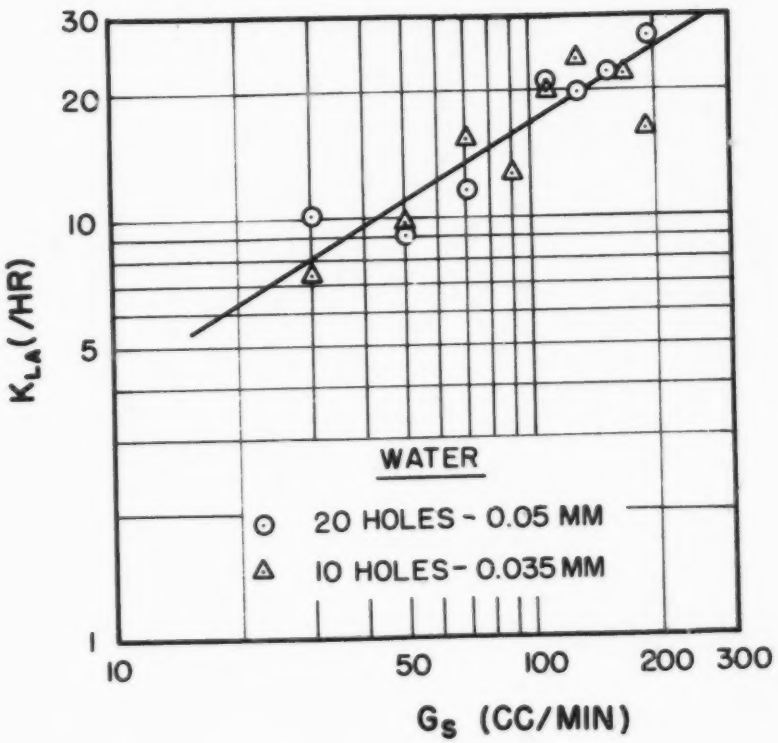

Figure 13 - Relationship Between the Overall Transfer Coefficient, $K_L a$, and Gas Flow for the Nylon Spinnerettes

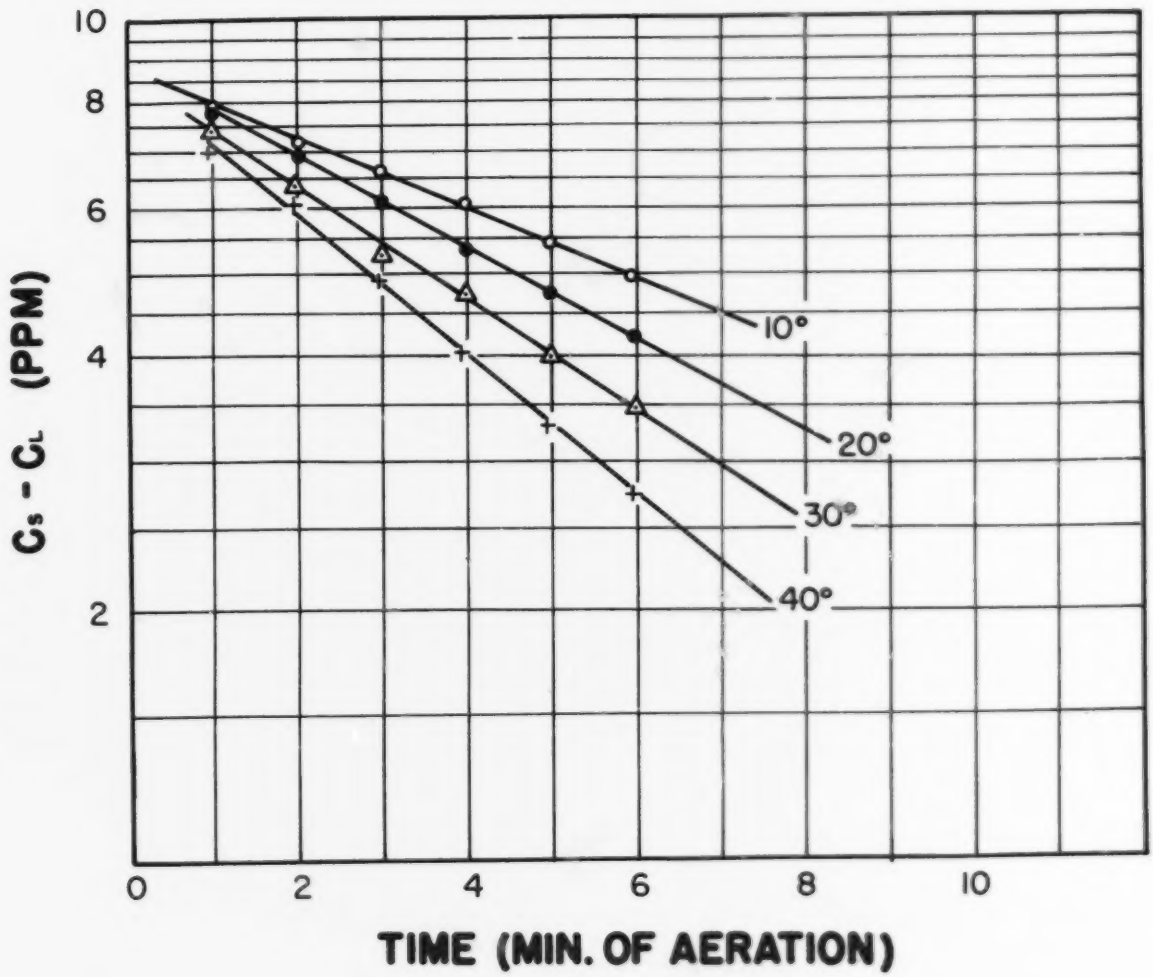

Figure 14 - A Typical Relationship for the Effect of Temperature on Oxygen Transfer

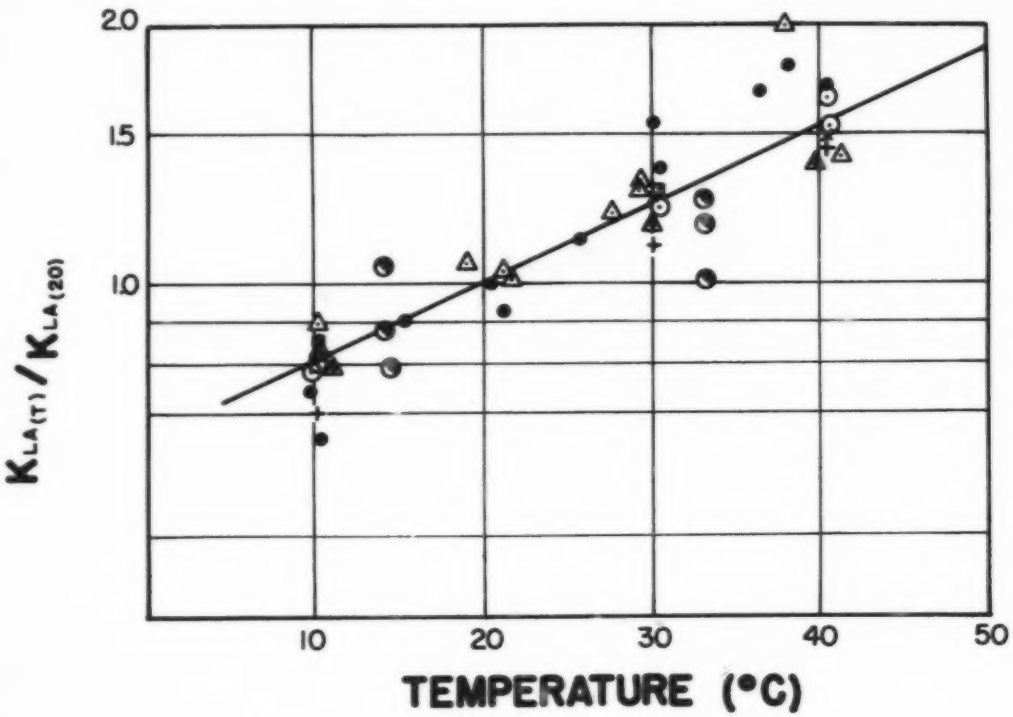

LEGEND

SYMBOL	SUBSTANCE	UNIT
⊙	WATER	SPIN. 20 HOLES; 0.035 MM.
+	"	" 10 HOLES; 0.05 MM.
●	"	ALOXITE STONE
△	1% KCl	" "
▣	1% KCl	SPIN. 10 HOLES; 0.05 MM.
×	50 PPM HEPTANOIC ACID	SPIN. 20 HOLES; 0.035 MM.
		DATA OF:
◔	WATER	CARPANI & REYBOUGH
▲	"	GAMESON ETAL

Figure 15 - Relationship Between the Overall Transfer Coefficient, $K_L a$, and Temperature

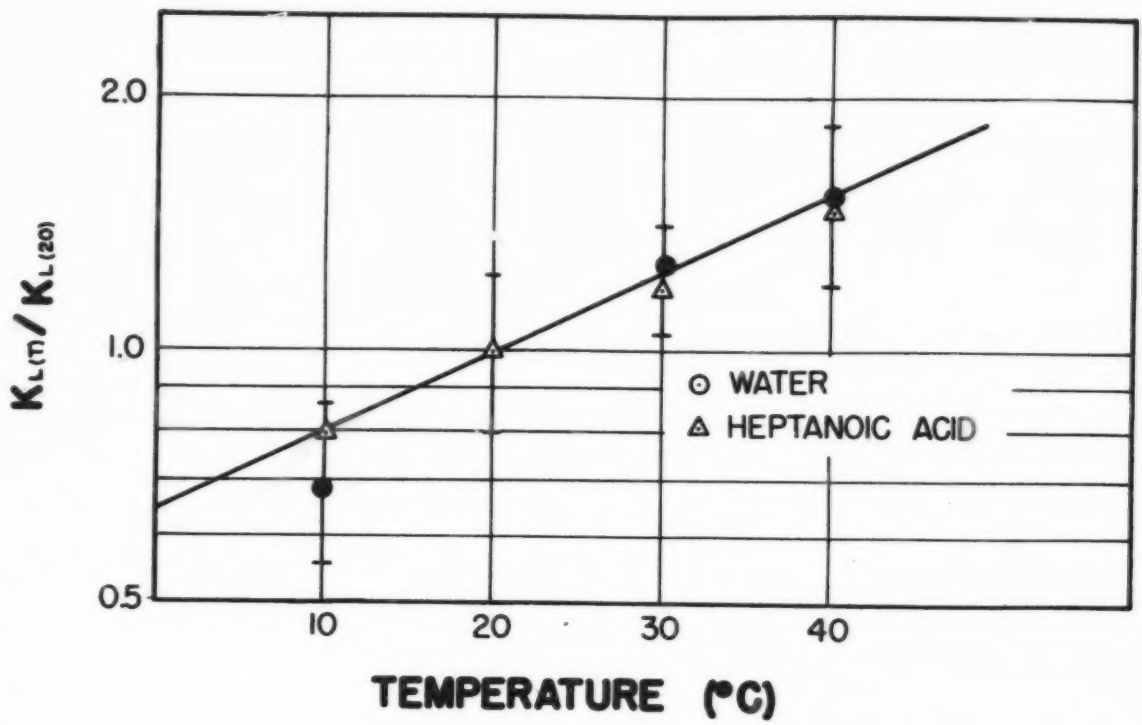

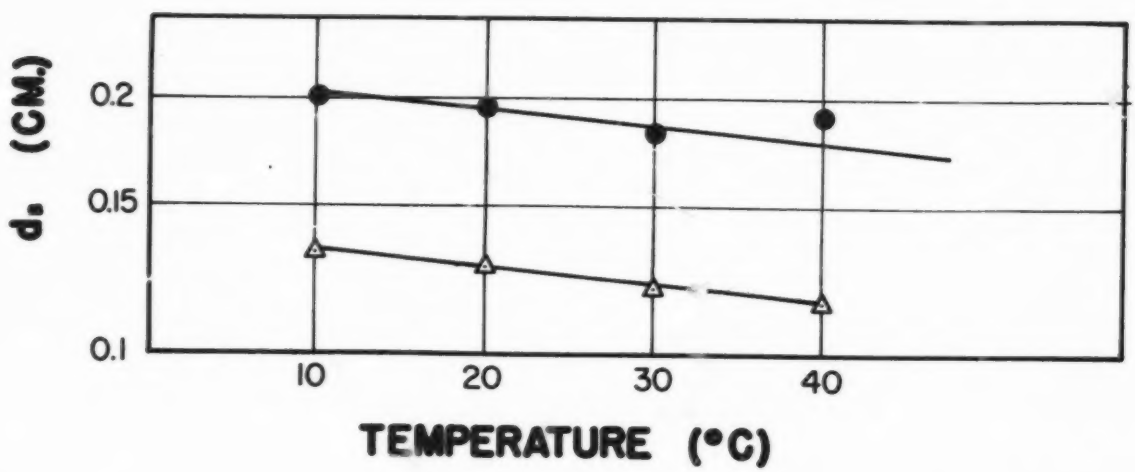

Figure 16 - Relationship Between Liquid Film Coefficient, K_L and Temperature

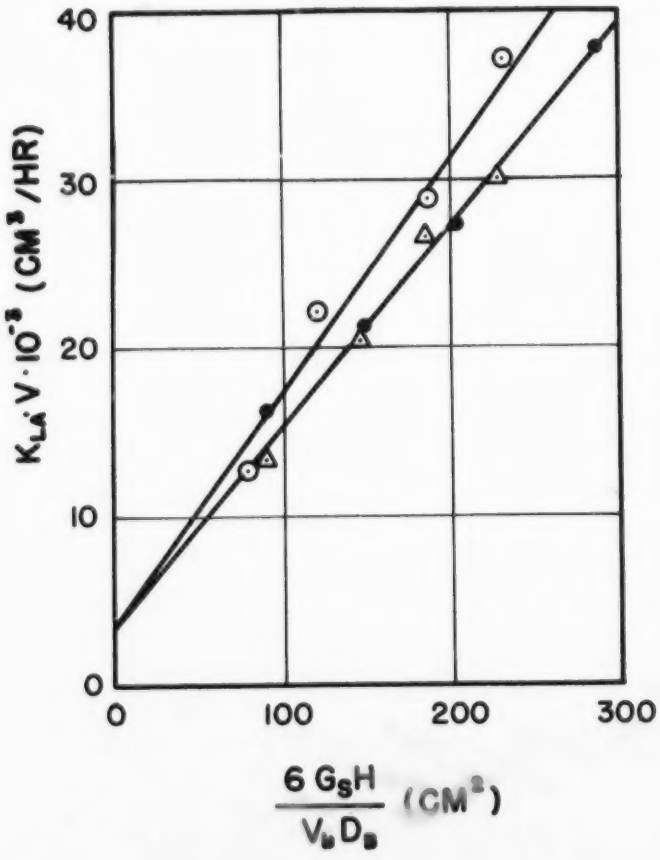

OUR DATA

RUN	SYMBOL	d_{BM} (CM)	V_{BM} (CM/SEC)
1	●	0.148	36.3
2	⊙	0.160	38.4
3	△	0.161	32.0

Figure 17 - Correlation to Develop End Effects for the Aeration Column

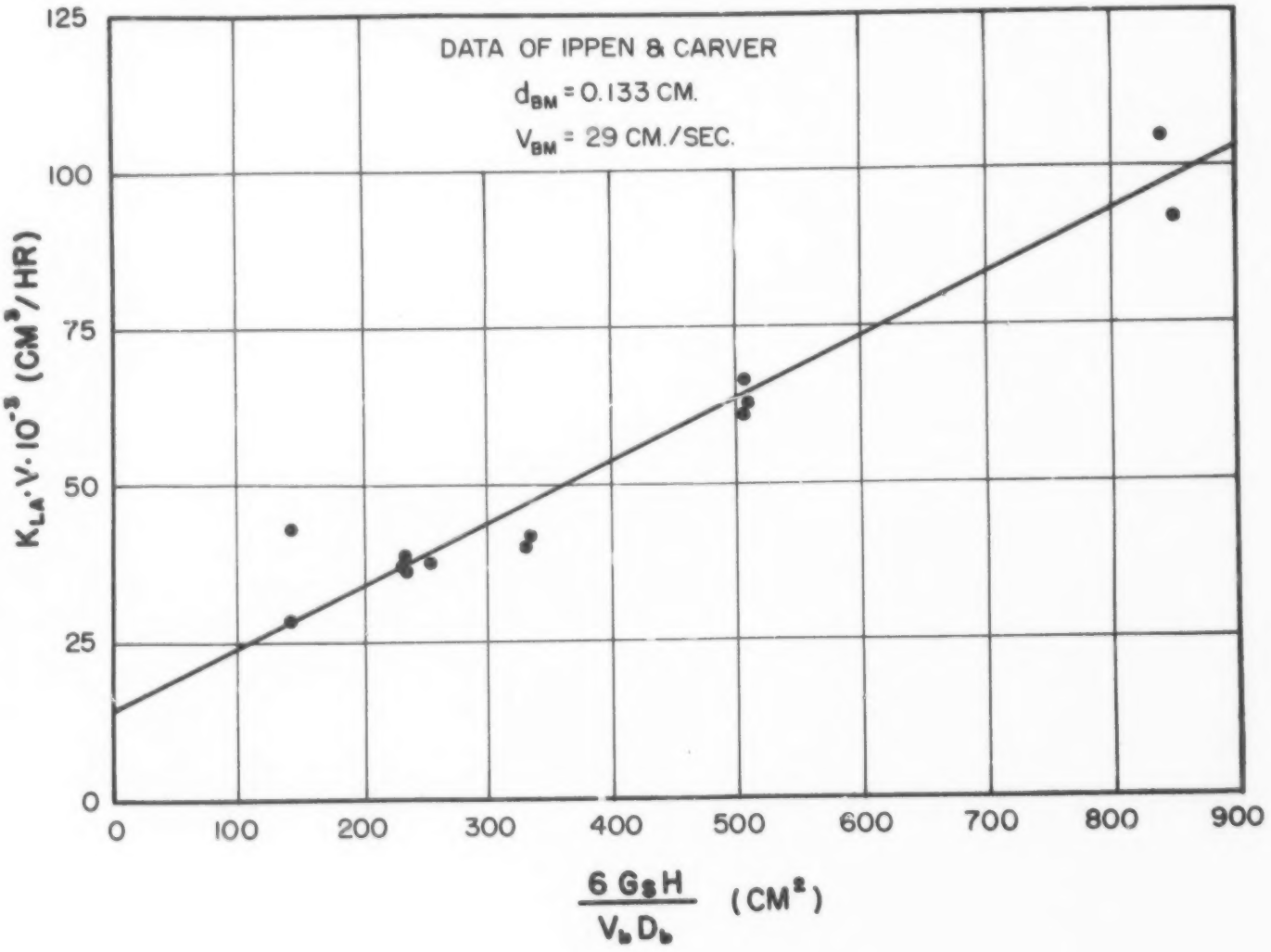

Figure 18 – End Effects from the Data of Other Investigators

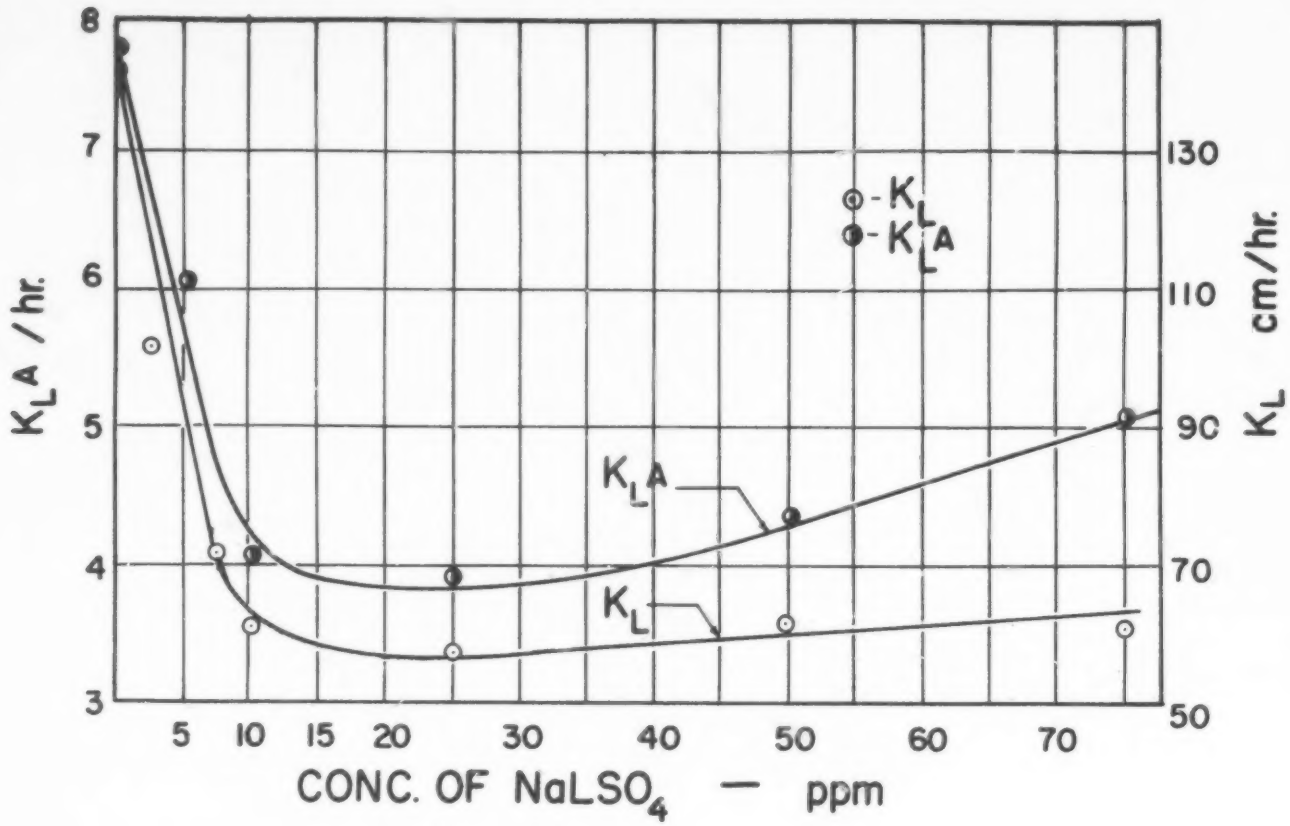

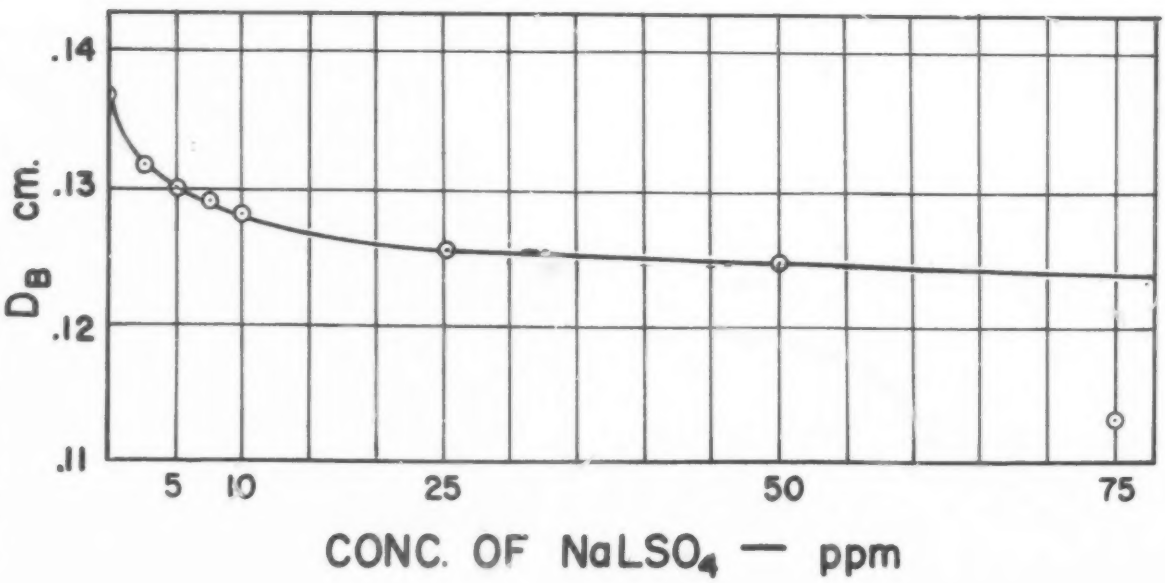

Figure 19 - Oxygen Transfer Characteristics in Dilute Solutions of Sodium Lauryl Sulfate

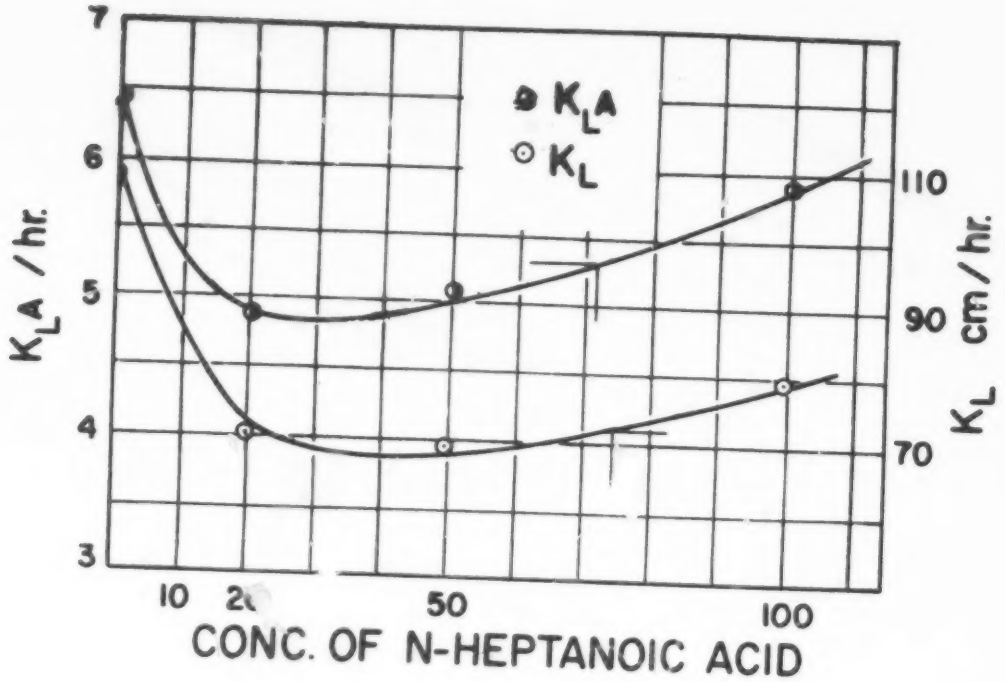

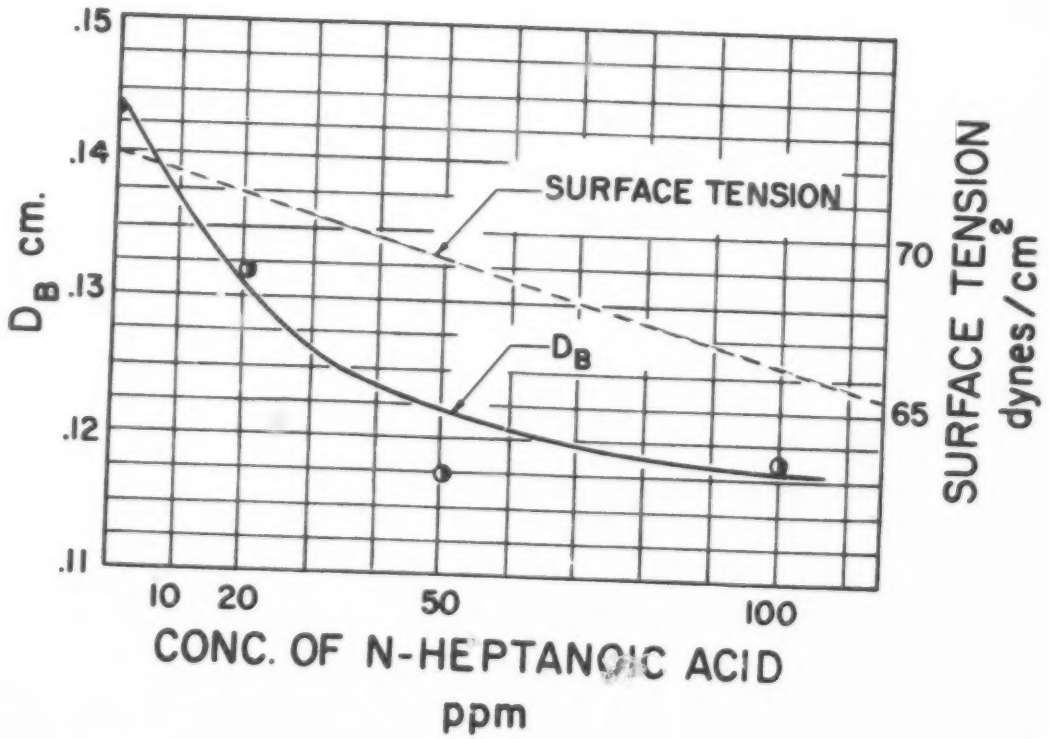

Figure 20 - Oxygen Transfer Characteristics in Dilute Solutions of Heptanoic Acid

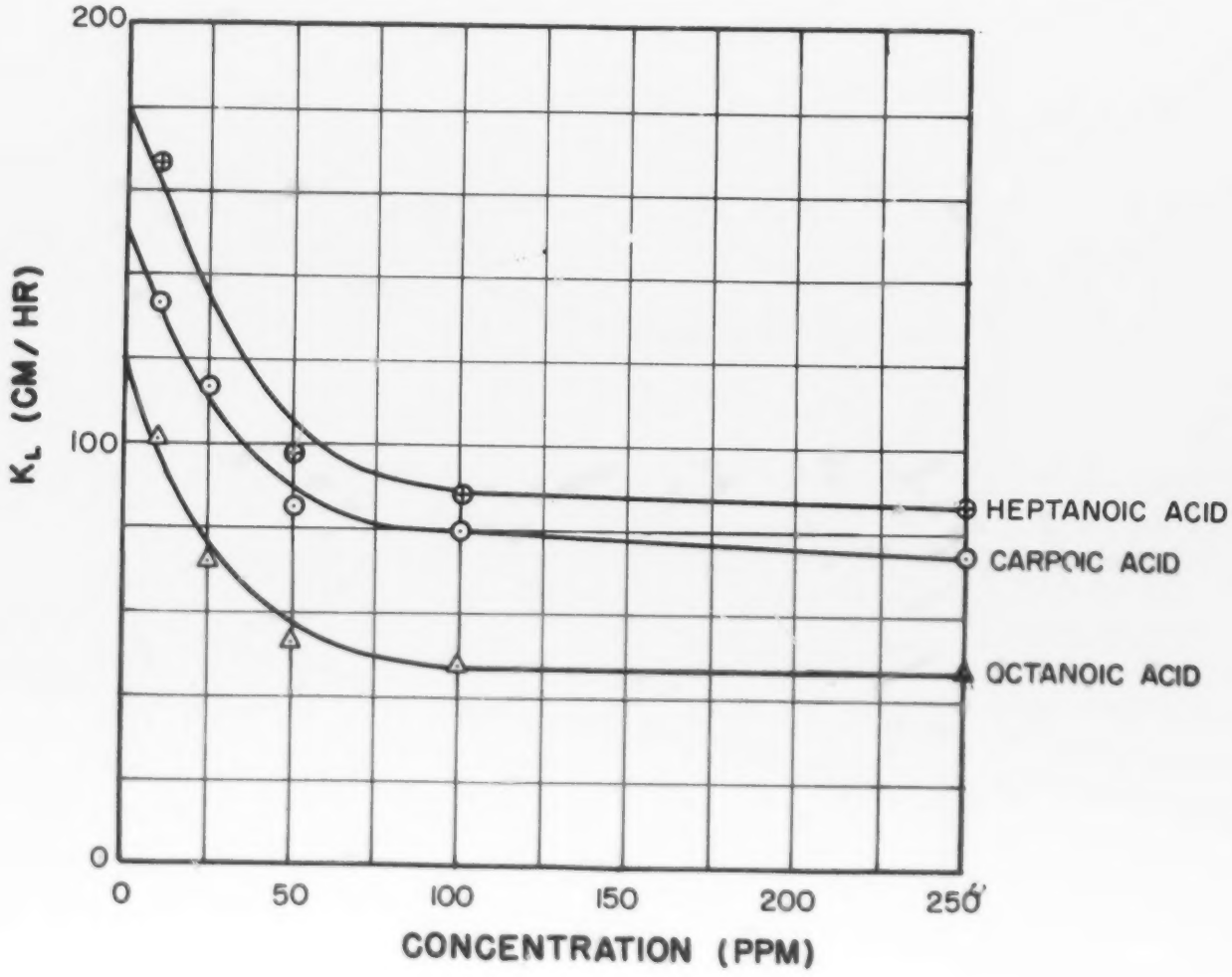

Figure 21 - Oxygen Transfer Characteristics of Dilute Solutions of Various Organic Acids